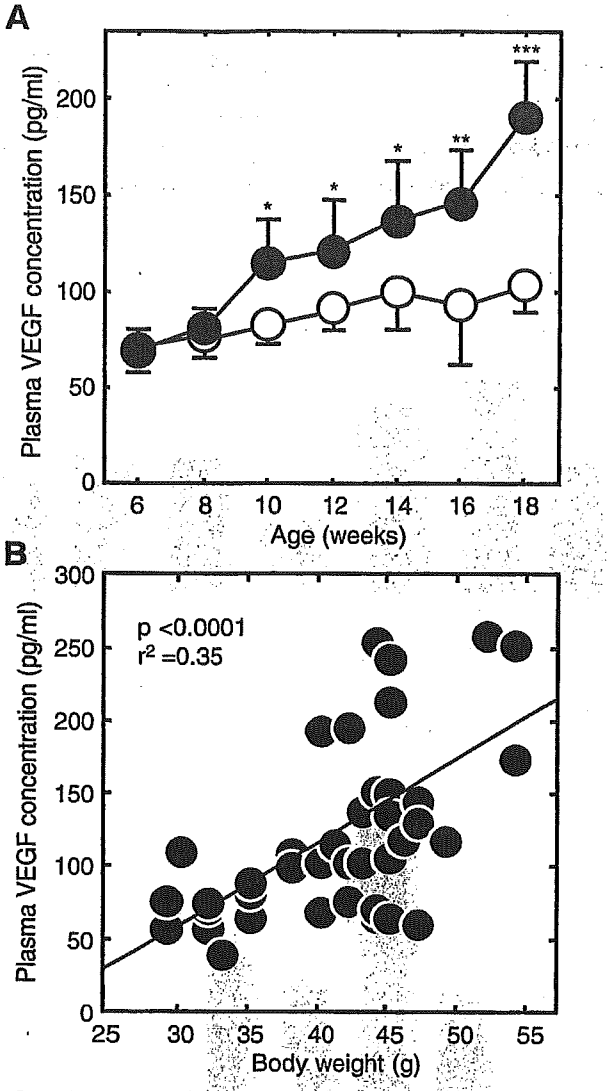

Fig. 1. Growth-dependent change of plasma vascular endothelial growth factor (VEGF) concentration in *db/db* mice. *A*: time course changes of plasma VEGF concentrations in *db/db* (●) and *db/+* (○) mice. Plasma VEGF concentrations were measured every 2 wk from 6 to 18 wk of age in *db/db* and *db/+* mice. Results are represented as means and SD. After 10 wk of age, plasma VEGF concentrations in *db/db* mice were significantly higher than in *db/+* mice. *B*: correlation between body weight and plasma VEGF concentrations in *db/db* mice. Plasma VEGF concentrations were significantly correlated with body weight in *db/db* mice. $*P < 0.05$ vs. *db/+* mice; $**P < 0.01$ vs. *db/+* mice; $***P < 0.001$ vs. *db/+* mice.

rodent chow (352 kcal/100 g, CE-2; CLEA Japan). Male mice were used in the studies reported here. Animal care and procedures were approved by the Animal Care Committee of Chiba University School of Medicine.

Body weight and adiposity. Body weights of *db/db* and *db/+* mice were measured at every 2 wk from the time they were 6 wk old throughout the study. Blood samples were also obtained from the retroorbital venous plexus of the mice fasted more than 16 h. The *db/db* and *db/+* mice were killed at 6, 10, 14, and 18 wk of age by cervical dislocation before white adipose tissues were collected. Mesenteric adipose tissues were used as visceral fat, and inguinal subcutaneous adipose tissues were used as subcutaneous fat in the studies reported here. The white adipose tissues were weighed on an analytic balance and processed for cell counts as described previously (13). Briefly, minced adipose tissues were incubated with PBS containing collagenase S-1. The tissue fragments were removed by passage through a 250-μm nylon screen. The isolated cells were then stained with methylene blue, and aliquots were placed on a Neubauer hemocytometer. Total cell counts were measured using a light microscope.

Total RNA and protein extraction from adipose tissues in obese mice. Mesenteric and subcutaneous adipose tissues of *db/db* and *db/+* mice were processed for total RNA isolation using ISOGEN reagents according to the manufacture's instructions. In another set of experiments, the adipose tissues were homogenized in an ice-cold buffer containing 50 mM Tris·HCl (pH 7.4), 1 mM EDTA, 1 mM dithiothreitol, 5 mM $MgCl_2$, 130 mM NaCl, 1% NP-40, 10 μM 4-amidinophenylmethanesulfonyl fluoride, and 5 μM leupeptin. Insoluble materials in the tissue were removed by centrifugation at 12,000 *g* at 4°C for 20 min. After centrifugation, tissue extracts were collected. Moreover, total RNA in the isolated adipocytes of mesenteric fat was also prepared. The mesenteric adipose tissue was digested with collagenase S-1 and passed through a 250-μm nylon screen to remove tissue debris. Then, the isolated cells, containing adipocytes and vascular-stromal cells, were separated by centrifugation. After the adipocytes were allowed to float, the vascular-stromal cells were removed from the bottom layer. The floating layer, as adipocyte fraction, was washed three times with PBS. Finally, the isolated adipocytes were collected and processed for cell counts, using a Neubauer chamber as described above. To compare directly the cellular expression of VEGF in adipocyte, 2×10^4 cells were processed for total RNA isolation using ISOGEN reagent. The KK-A^y and C57BL/6 mice were killed at 16 wk of age by cervical dislocation before mesenteric and inguinal subcutaneous fat was collected for total RNA isolation.

3T3-L1 cells culture and differentiation. 3T3-L1 preadipocytes were cultured with DMEM containing 10% FBS at 37°C in a 5% CO_2 incubator. Adipocyte differentiation was carried out by changing to a differentiation medium containing 10 μg/ml insulin, 0.25 μM dexamethasone, and 0.5 mM 3-isobutyl-1-methylxanthine. After 48 h, the medium was replaced with a maturation medium containing 5 μg/ml insulin, and cells were maintained in this medium until use. Every week after differentiation, the cells were washed with PBS and then cultured in fresh DMEM medium alone. After incubation for 24 h, the conditioned media were collected. In another set of experiments, the cells were processed for total RNA isolation using an RNeasy Mini Kit.

In vitro endothelial tube formation assay. HUVECs were grown in EBM-2 medium containing 10% FBS. Formation of capillary tube-like structures by HUVECs was assessed in a Matrigel-based assay as previously described (8). Briefly, HUVECs were incubated with MCDB131 containing 2% FBS for 48 h prior to tube formation assay. Cells (7×10^4) were plated onto 300 μl of Growth Factor Reduced BD Matrigel matrix (7 mg/ml protein), pregelled at 37°C in 24-well culture plates. Then, the cells were incubated for 13 h at 37°C with 150 μl of MCDB131 and 150 μl of the conditioned medium derived from pre- or postdifferentiated 3T3-L1 cells in the presence or absence of anti-mouse VEGF-neutralizing antibody. Three different phase-contrast microscopic low-power fields (×100) per well were photographed. The total length of capillary tubes in each photograph was measured using a scale ruler.

Preadipocyte transplantation. 3T3-L1 cells were implanted into athymic mice as described previously (19). Briefly, 3T3-L1 preadipocytes were grown to near confluence, trypsinized, and suspended in DMEM with 10% FBS. After centrifugation, cell pellets were resuspended in PBS and injected 1×10^7 cells (500 μl) through 22-gauge needles into the mesenteric area near the small intestine or the subcutaneous fat area of athymic mice of the BALB/C strain under

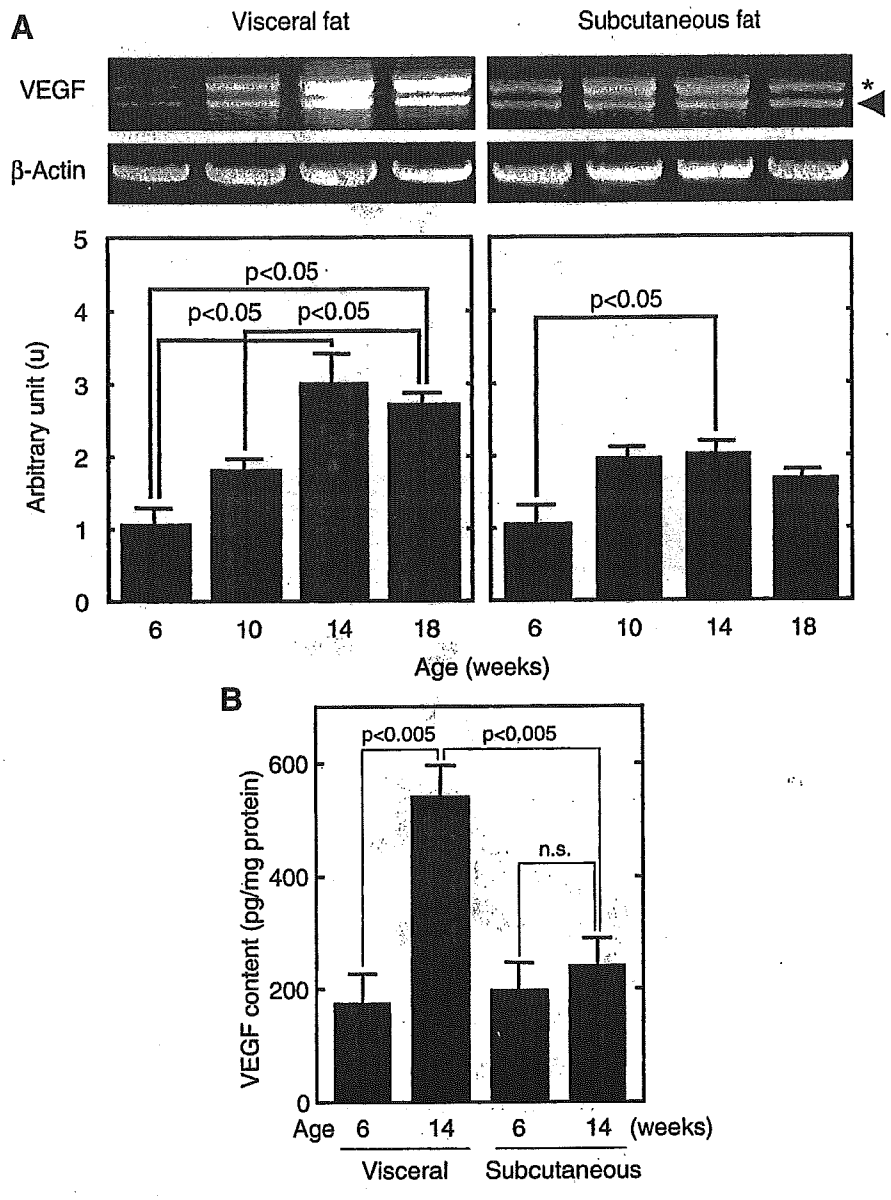

Fig. 2. Growth-dependent changes of mRNA expressions and protein contents of VEGF in mesenteric and subcutaneous adipose tissues of *db/db* mice. *A*: Time course changes of VEGF gene expressions in visceral and subcutaneous adipose tissues of *db/db* mice. Images show RT-PCR products of VEGF amplified from total RNA in mesenteric and subcutaneous adipose tissues at 6, 10, 14, and 18 wk after birth. PCR products of VEGF were densitometrically analyzed, and relative amounts at 6 wk old were set to 1.0. Results are represented as means and SD. Arrowhead, 644 bp ($VEGF_{164}$); *, 716 bp ($VEGF_{188}$). *B*: Tissue VEGF contents in mesenteric and subcutaneous fat. Tissues were extracted with a buffer containing 50 mmol/l Tris·HCl (pH 7.4), 1 mmol/l EDTA, 1 mmol/l DTT, 5 mmol/l $MgCl_2$, 130 mmol/l NaCl, 1% NP-40, 10 μmol/l APMSF, and 5 μmol/l leupeptin. Tissue extracts were processed for VEGF measurement using an ELISA system.

anesthetization by intraperitoneal injection with pentobarbital sodium. Mice were housed in microisolator cages under specific pathogen-free conditions during whole experiments. Four weeks after implantation, the mice were killed by cervical dislocation under anesthetization before mesenteric or subcutaneous fat area was collected. Total RNA of mesenteric and subcutaneous fat was isolated using ISOGEN reagent. Blood samples were also obtained from the retroorbital venous plexus of the mice fasted more than 16 h.

Measurement of immunoreactive VEGF. Plasma samples were prepared by centrifugation at 1,500 *g* for 15 min at 4°C. After centrifugation, the plasma fraction was collected and stored at −70°C until use. The extracts of adipose tissues and the conditioned media from pre- and postdifferentiated 3T3-L1 cells were also stored at −70°C until use. VEGF concentrations of plasma, extracts from adipose tissues, and conditioned media were measured with an enzyme-linked immunosorbent assay system (R&D Systems, Minneapolis, MN).

RT-PCR. To evaluate the contents of VEGF expression in adipose tissues and 3T3-L1 cells, 0.4 μg of total RNA was amplified by OneStep RT-PCR kit using the indicated specific primers. To compare directly the VEGF expressions in adipocytes of mesenteric fat during growth, total RNA prepared from 2×10^4 cells was also amplified using the specific primers. The contents of GLUT4, peroxisome proliferator-activated receptor-γ (PPARγ), and β-actin were also amplified by RT-PCR. The RT-PCR products were run on 1.5% agarose and stained with ethidium bromide. The relative signal intensities of the PCR products were determined with luminescent image analyzer LAS-1000 (Fuji Photo Film, Tokyo, Japan). mRNA amounts were normalized to levels of β-actin mRNA, which served as endogenous standard.

Primers. The following primers were designed for RT-PCR analysis using in this study: VEGF, 5′-GCGGGCTGCCTCGCAGTC-3′ (forward) and 5′-TCACCGCCTTGGCTTGTCAC-3′ (reverse); β-actin, 5′-TGGAATCCTGTGGCATCCATGAAAC-3′ (forward) and 5′-TAAAACGCAGCTCAGTAACAGTCCG-3′ (reverse); GLUT4, 5′-GGCATGTGTGGCTGTGCCATC-3′ (forward) and 5′-GGGTTTCACCTCCTGCTCTAA-3′ (reverse); PPARγ, 5′-GACATCCAA-

GACAACCTGCTG-3′ (forward) and 5′-GCAATCAATAGAAG-GAACACG-3′ (reverse). RT-PCR products for VEGF were 716 bp ($VEGF_{188}$), 644 bp ($VEGF_{164}$), and 512 bp ($VEGF_{120}$), respectively. The signal intensity of the 644-bp product was analyzed in this study. Products of 349, 413, and 258 bp were predicted for β-actin, GLUT4, and PPARγ, respectively.

Statistical analysis. Statistical analyses were performed using Statview J-4.5. Statistical analysis was performed with a *t*-test. All of the results reported herein were confirmed by repeating the experiments with different occasions. A value of $P < 0.05$ indicated statistical significance.

RESULTS

Growth-dependent changes of plasma VEGF concentration in db/db mice. We measured circulating VEGF concentrations in *db/db* mice, a strain of the mouse models for obesity, to demonstrate the role of fat accumulation and its effect on VEGF levels in vivo. Plasma VEGF concentrations were increased during growth in both *db/+* and *db/db* mice (Fig. 1*A*). At 10 wk old, plasma VEGF concentrations in *db/db* mice were significantly higher than in *db/+* mice. Moreover, plasma VEGF concentrations were significantly correlated with body weight (Fig. 1*B*).

Growth-dependent changes of VEGF mRNA expressions and protein contents in visceral and subcutaneous fat of db/db mice. VEGF mRNA was detected in both visceral and subcutaneous fat in *db/db* mice. Expression levels of VEGF mRNA in visceral fat were increased 3.0-fold in 14-wk-old mice compared with those in 6-wk-old mice (Fig. 2*A*). VEGF expressions in subcutaneous fat were also increased during growth, but its enhancement was smaller than in visceral fat. Moreover, tissue contents of VEGF in visceral fat were significantly increased in 14-wk-old mice compared with those in 6-wk-old mice (Fig. 2*B*). However, the VEGF contents in subcutaneous fat were almost the same in 6- and 14-wk-old mice. These data suggest that an enhanced expression of the VEGF gene in visceral fat mainly contributes to the elevated plasma concentrations.

Effect of fat accumulation on VEGF expression in white adipose tissues of db/db mice. Whole tissue weights of mesenteric and subcutaneous fat were increased gradually during growth (Fig. 3*A*). Total cell counts were significantly decreased during growth only in mesenteric adipose tissues (Fig. 3*B*). A significant correlation between fat weight and VEGF expression levels was observed in mesenteric adipose tissue but not in subcutaneous adipose tissue (Fig. 4*A*). Moreover, cellular levels of VEGF expression were calculated from the results of mRNA expression levels and total cell counts in adipose tissues and positively correlated for adiposity in mesenteric adipose tissue but not in subcutaneous adipose tissue (Fig. 4*B*).

Growth-dependent change of VEGF expression in adipocytes of visceral area of db/db mice. VEGF expressions in adipocyte fraction were increased during growth (Fig. 5). Cellular expression levels of VEGF mRNA in visceral adipocytes were increased sevenfold in 18-wk-old mice compared

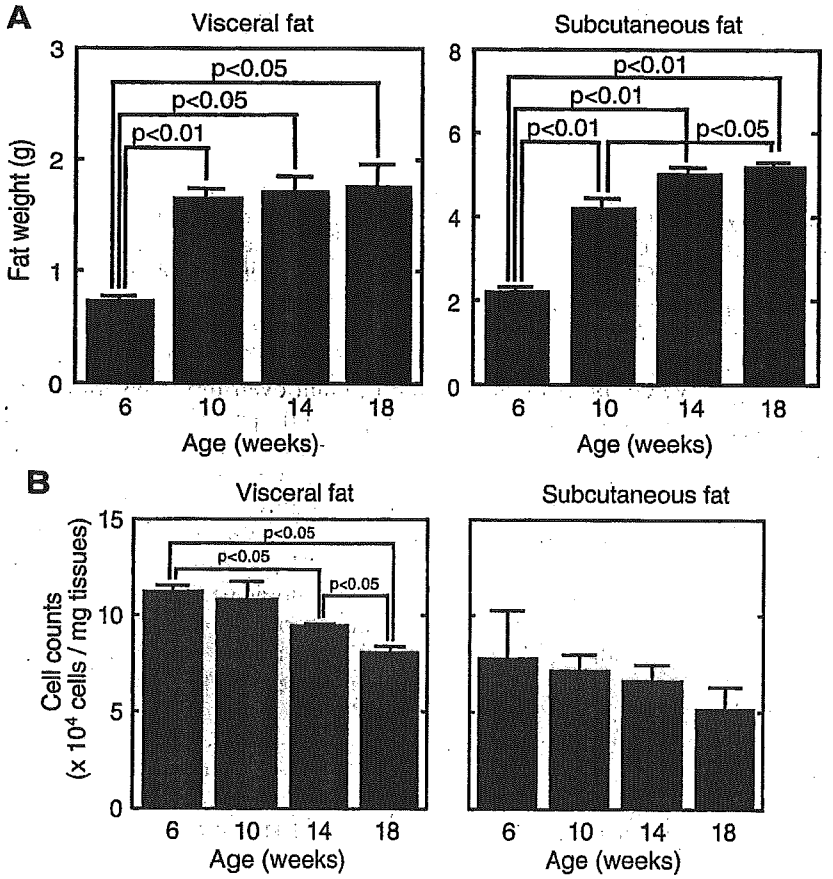

Fig. 3. Growth-dependent changes of fat weight and adiposity in mesenteric and subcutaneous adipose tissues. *A*: Time course changes of mesenteric and subcutaneous adipose tissue weights in *db/db* mice. The *db/db* mice were killed by cervical dislocation at 6, 10, 14, and 18 wk of age before adipose tissues were collected. Mesenteric and subcutaneous fat was weighed on an analytic balance. Results are represented as means + SD. *B*: Time course change of adiposity of mesenteric and subcutaneous adipose tissues in *db/db* mice. Mesenteric and subcutaneous fat was digested with collagenase S-1 and processed for cell counts using a Neubauer chamber. Results are represented as means + SD.

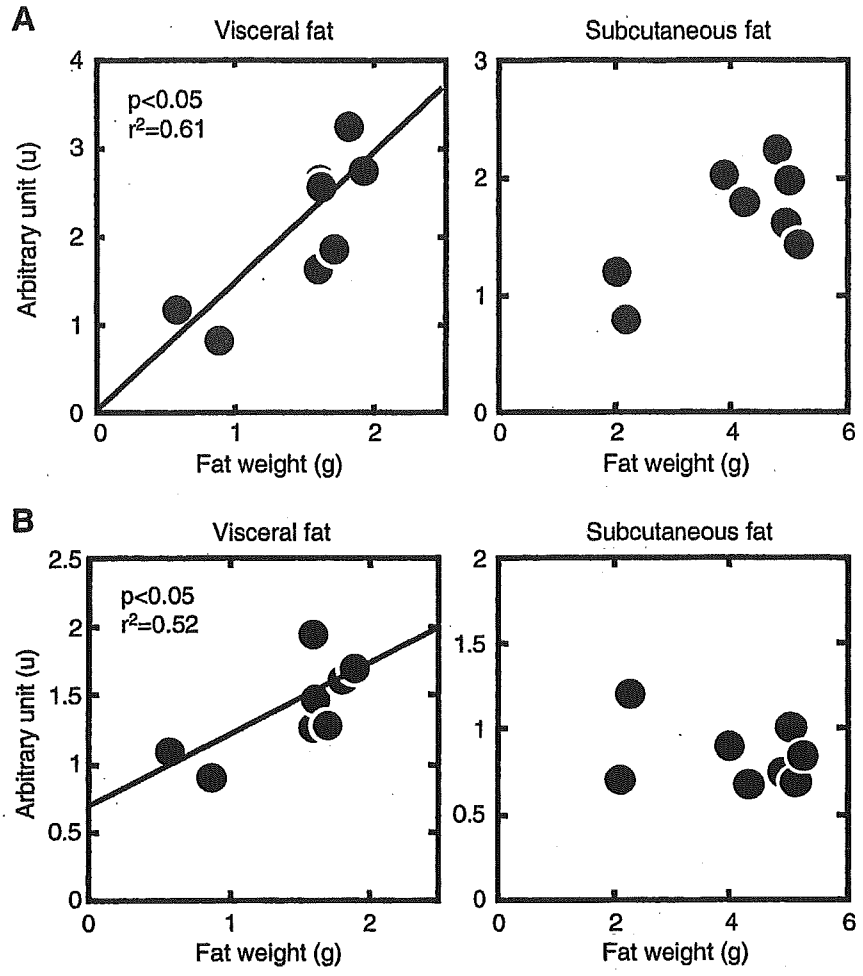

Fig. 4. Correlation between fat weight or adiposity and VEGF expressions in mesenteric adipose tissue. *A*: positive correlation between fat weight and tissue VEGF expression in mesenteric adipose tissues. *B*: positive correlation between fat weight and cellular VEGF expression in mesenteric adipose tissues.

with those in 6-wk-old mice. These results suggest that circulating VEGF concentrations in *db/db* mice were increased by the enhancement of VEGF mRNA expression in visceral adipocytes.

Plasma concentration and tissue expression of VEGF in KK-A^y mice. To demonstrate the correlation between VEGF expression and adiposity in another model of obesity, we analyzed KK-A^y mice. Plasma VEGF concentrations were significantly increased in both 8- and 16-wk-old KK-A^y mice compared with those in age-matched control mice (Fig. 6*A*). Moreover, expression levels of VEGF mRNA in visceral fat were significantly increased in KK-A^y mice compared with those in control mice (Fig. 6*B*). These results suggest that circulating VEGF concentrations in KK-A^y mice as well as in *db/db* mice were increased by the enhancement of VEGF mRNA expression in visceral fat.

Change of VEGF expressions during differentiation and maturation process in 3T3-L1 cells. We performed RT-PCR analysis for the gene expression of VEGF, PPARγ, and GLUT4 in cultured 3T3-L1 cells. VEGF mRNA was expressed even in the preadipocyte condition (Fig. 7*A*), and its expression was enhanced during adipocyte conversion. Especially, the expression levels of VEGF mRNA were significantly increased 14 days after differentiation (Fig. 7*B*). Both PPARγ and GLUT4 expressions were gradually enhanced during differentiation (Fig. 7*A*). These results suggest that expression levels of VEGF mRNA in 3T3-L1 cells were enhanced during lipid accumulation.

VEGF concentrations of conditioned media cultured with pre- and postdifferentiated 3T3-L1 cells. 3T3-L1 cells secreted VEGF proteins into culture medium even in the preadipocyte condition (Table 1), and the VEGF protein secretion was enhanced during adipocyte conversion. Especially, the VEGF concentrations in conditioned medium were increased fourfold 14 days after differentiation compared with those of predifferentiation. These results suggest that protein secretion as well as mRNA expression of VEGF in 3T3-L1 cells were enhanced during lipid accumulation. The biological activity of VEGF should be examined to know the role of VEGF in physiological and pathological conditions. Therefore, we demonstrated the angiogenic activity of conditioned medium from cultured adipocytes.

Enhancement of tube formation activity in HUVECs by addition of conditioned medium cultured with 3T3-L1 cells. VEGF secreted from both pre- and postdifferentiated 3T3-L1 cells had stimulatory activity toward HUVECs in tube formation (Fig. 8, *A* and *B*). The stimulatory activity in the condi-

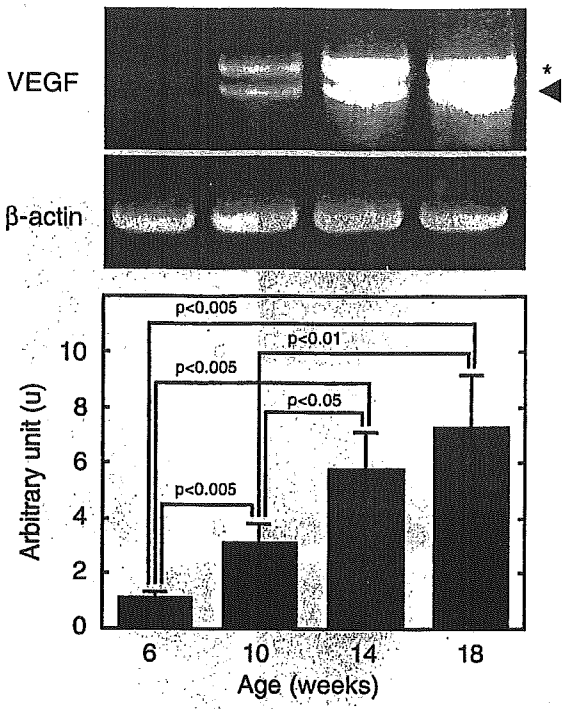

Fig. 5. Time course change of VEGF expressions in adipocyte fraction prepared from mesenteric fat of *db/db* mice. Visceral fat was cut into small pieces and digested using collagenase S-1. Then, the tissues were suspended with PBS and separated by centrifugation. The floating layer was collected as adipocyte fraction. Images show RT-PCR products of VEGF amplified from total RNA prepared from 2×10^4 cells of adipocytes at 6, 10, 14, and 18 wk after birth. The PCR products of VEGF were densitometrically analyzed, and the relative amounts at 6 wk old were set to 1.0. Results are represented as means and SD. Arrowhead, $VEGF_{164}$; *, $VEGF_{188}$.

tioned medium derived from postdifferentiated 3T3-L1 cells was three times higher than in predifferentiated cells. Moreover, anti-VEGF-neutralizing antibody apparently inhibited the stimulatory tube formation activity in both pre- and postdifferentiated 3T3-L1 cells. These findings suggest that 3T3-L1 cells secrete the bioactive form of VEGF protein.

Effect of implantation of 3T3-L1 preadipocytes into mesenteric or subcutaneous fat area of nude mice on VEGF expression. We performed RT-PCR analysis for gene expressions of VEGF, PPARγ, and GLUT4 in the mesenteric or subcutaneous fat area implanted with 3T3-L1 cells. As shown in Fig. 9*A*, the content of VEGF expression was increased fourfold in the mesenteric fat implanted with 3T3-L1 cells compared with those in sham-operated control mice. In contrast, VEGF expression of subcutaneous fat was almost the same in the mice implanted with 3T3-L1 cells into the subcutaneous area and controls. Moreover, PPARγ expression was enhanced only in mesenteric fat implanted with 3T3-L1 cells but not in subcutaneous fat. The expression levels of GLUT4 in both mesenteric and subcutaneous fat implanted with 3T3-L1 cells were higher than in controls.

The plasma VEGF concentration increased after implantation with 3T3-L1 cells into the mesenteric area, and these reached 381 ± 63 pg/ml at 4 wk. However, the mice injected in the subcutaneous area did not show any difference from control mice (Fig. 9*B*).

DISCUSSION

In the first set of experiments, we showed that the plasma VEGF concentrations gradually increased during growth in both *db/db* and *db/+* mice. After 10 wk of age, however, plasma VEGF concentrations were higher in *db/db* mice than in *db/+* mice. The *db/db* mice are considered to be an obesity model because fat deposition is the primary change. Then we analyzed the correlation between plasma VEGF concentration and body weight. The plasma VEGF concentration in *db/db*

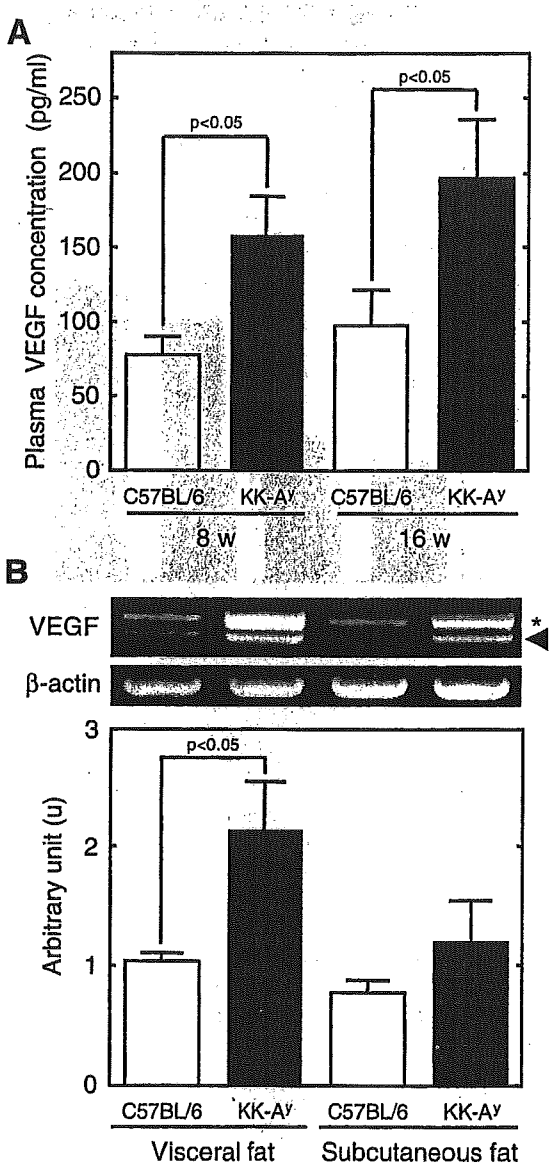

Fig. 6. Plasma concentration and tissue expression of VEGF in KK-A^y mice. *A*: comparison of plasma VEGF concentrations between KK-A^y and C57BL/6 mice. Plasma VEGF concentrations were measured in 8- and 16-wk-old KK-A^y and C57BL/6 mice. Results are represented as means + SD. *B*: comparison of VEGF gene expressions in visceral and subcutaneous adipose tissues between KK-A^y and C57BL/6 mice. Images show RT-PCR products of VEGF amplified from total RNA in mesenteric and subcutaneous adipose tissues at 16 wk after birth. The PCR products of VEGF were densitometrically analyzed, and the relative amounts in visceral adipose tissues of control mice were set to 1.0. Results are represented as means + SD. Arrowhead, $VEGF_{164}$; *, $VEGF_{188}$.

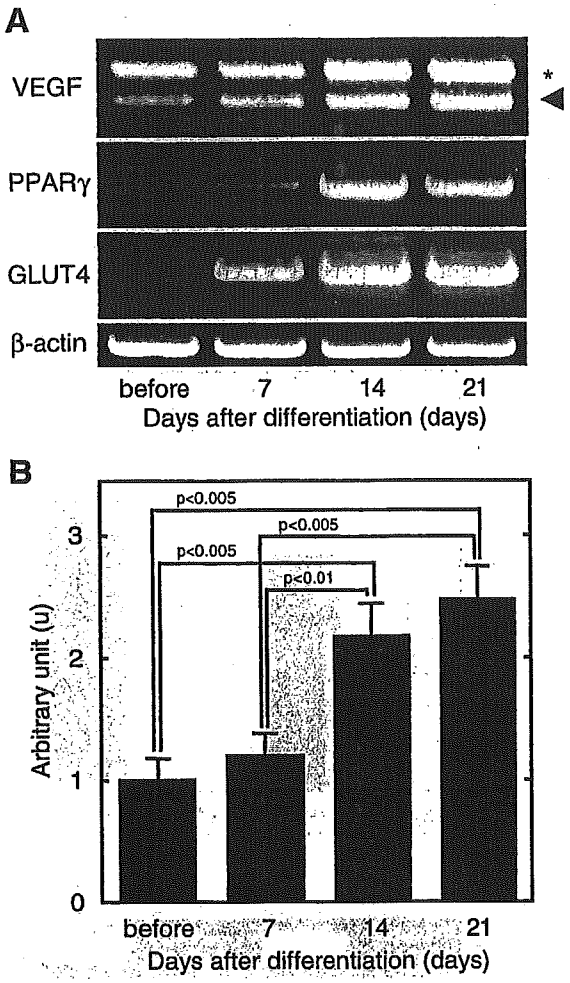

Fig. 7. Time course changes of VEGF, peroxisome proliferator-activated receptor-γ (PPARγ), and GLUT4 expressions in 3T3-L1 cells during adipocyte differentiation. *A*: gene expression profiles in 3T3-L1 cells during adipocyte differentiation. Images show RT-PCR products of VEGF, PPARγ, and GLUT4 amplified from total RNA in 3T3-L1 cells at 0, 7, 14, and 21 days after differentiation. *B*: relative amounts of VEGF expressions in 3T3-L1 cells during adipocyte differentiation. The PCR products of VEGF were densitometrically analyzed, and the relative amounts in predifferentiated 3T3-L1 cells were set to 1.0. Results are represented as means + SD. Arrowhead, $VEGF_{164}$; *, $VEGF_{188}$.

mice was significantly related to their body weight, the same as our previous results in human subjects (15). These results suggest that plasma VEGF may be determined by body fat deposition in mice.

In our previous report (15), plasma VEGF concentrations were revealed to be dependent on visceral fat accumulation. Therefore, to clarify the VEGF expressions with regard to whether subcutaneous or visceral adipose tissue affects plasma VEGF concentration in *db/db* mice, we examined mRNA expressions and protein contents of VEGF in visceral and subcutaneous adipose tissues during growth. The mRNA ex-

Table 1. *VEGF concentrations of conditioned media cultured with pre- and postdifferentiated 3T3-L1 cells*

Differentiation periods	Days 0	7	14	21
VEGF concentration, ng/ml	0.6±0.1	0.9±0.2	2.4±0.5	2.6±0.2
Total protein concentration, mg/ml	0.4±0.1	0.4±0.1	0.4±0.2	0.4±0.2

Values are means ± SD. VEGF, vascular endothelial growth factor.

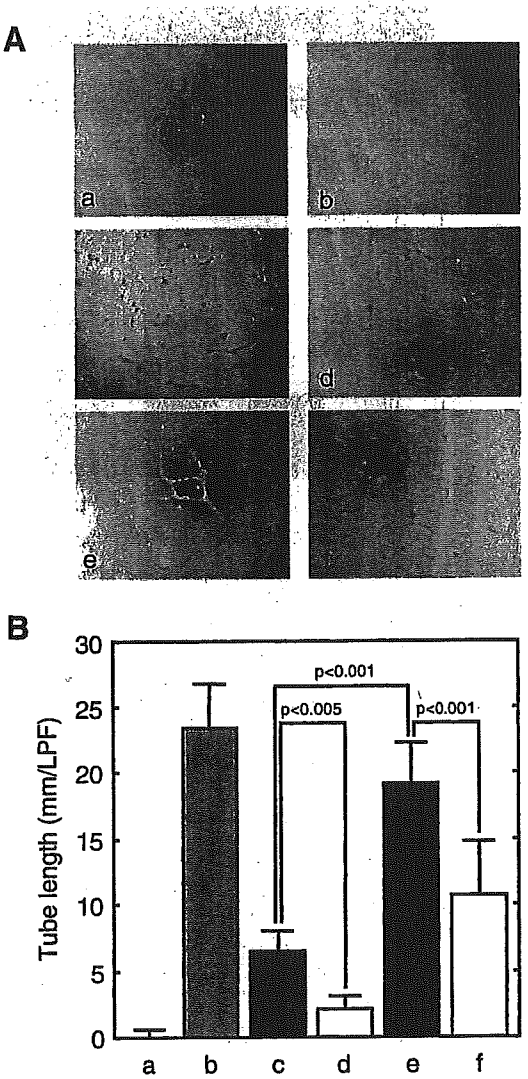

Fig. 8. Effect of conditioned media cultured with pre- and postdifferentiated 3T3-L1 cells on tube formation activity in human umbilical vein endothelial cells (HUVECs). *A*: light microscopic findings of tube formation of HUVECs in various conditions. Formation of capillary tube-like structures by HUVECs was assessed in a Matrigel-based assay as previously described (8). HUVECs were seeded on Growth Factor Reduced BD Matrigel matrix with conditioned medium derived from pre- or postdifferentiated 3T3-L1 cells in the presence or absence of anti-mouse VEGF-neutralizing antibody or recombinant VEGF protein. After 13 h of stimulation, phase-contrast microscopic low-power fields (×100) were photographed. *a*: medium alone; *b*: stimulated with recombinant VEGF (5 ng/ml); *c* and *d*: with conditioned medium from predifferentiated 3T3-L1 cells; *e* and *f*: with conditioned medium from postdifferentiated 3T3-L1 cells; *c* and *e*: in the absence of anti-VEGF antibody; *d* and *f*: in the presence of anti-VEGF antibody. *B*: tube length of HUVECs stimulated with conditioned medium prepared from pre- or postdifferentiated 3T3-L1 cells. The total length of capillary tubes formed by HUVECs in 3 different photographs per well were measured using a scale ruler. *Bar a*, medium alone; *bar b*, recombinant VEGF (5 ng/ml); *bar c*, conditioned medium from predifferentiated 3T3-L1 cells alone; *bar d*, conditioned medium from predifferentiated 3T3-L1 cells with anti-VEGF antibody; *bar e*, conditioned medium from postdifferentiated 3T3-L1 cells alone; *bar f*, conditioned medium from postdifferentiated 3T3-L1 cells with anti-VEGF antibody.

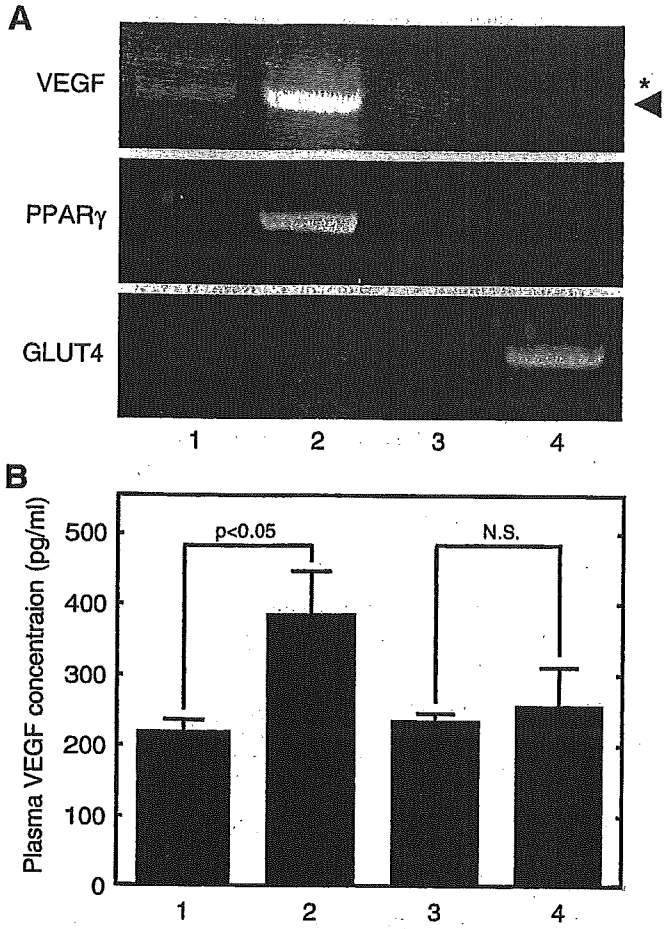

Fig. 9. Comparison of VEGF, PPARγ, and GLUT4 expressions among mice implanted with 3T3-L1 cells into mesenteric or subcutaneous fat area and controls. *A*: gene expression profiles in 3T3-L1 cells implanted into adipose tissues of nude mice. Images show RT-PCR products of VEGF, PPARγ, and GLUT4 amplified from total RNA in adipose tissues. *Lane 1*, mesenteric adipose tissues injected with PBS alone; *lane 2*, mesenteric adipose tissues injected with 3T3-L1 cells; *lane 3*, subcutaneous adipose tissues injected with PBS alone; *lane 4*, subcutaneous adipose tissues injected with 3T3-L1 cells. Arrowhead, $VEGF_{164}$; *, $VEGF_{188}$. *B*: plasma VEGF concentrations in mice implanted with 3T3-L1 cells. Plasma VEGF concentrations were measured at 4 wk after implantation with 3T3-L1 cells. *Lane 1*, mice injected with PBS alone into mesenteric area; *lane 2*, mice injected with 3T3-L1 cells into mesenteric area; *lane 3*, mice injected with PBS alone into subcutaneous area; *lane 4*, mice injected with 3T3-L1 cells into subcutaneous area.

pression levels of VEGF in visceral fat were more enhanced than in subcutaneous fat. Furthermore, the protein contents were enhanced in visceral fat but not in subcutaneous fat. These results suggest that plasma VEGF concentrations are revealed to be dependent on visceral fat accumulation even in mice.

The expression levels of TNF-α and PAI-1 in adipocytes are reported to be directly related to the degree of differentiation from preadipocytes and to be dependent on their anatomic location (12, 14, 20, 21). Therefore, we demonstrated the degree of fat accumulation in adipocytes and the correlation between VEGF mRNA expressions and adiposity in subcutaneous and mesenteric adipose tissues. Whole tissue weights of mesenteric and subcutaneous fat were increased gradually during growth. However, total cell counts were significantly decreased during growth in mesenteric fat but not in subcutaneous fat. A significant correlation between VEGF mRNA expressions and weight and adiposity in mesenteric adipose tissue was observed, but not in subcutaneous adipose tissue. These results suggest that the increase of weight in mesenteric adipose tissue is dependent on fat accumulation in adipocytes but not in subcutaneous adipose tissue. Moreover, VEGF expression is dependent on the levels of fat deposition in adipocytes. Then, we isolated the adipocyte fraction from mesenteric fat and examined VEGF mRNA expression in adipocytes. VEGF expression levels in the adipocyte fraction were also increased during growth.

Next, we examined the relation between VEGF expression and degree of differentiation using 3T3-L1 cells, an established adipocyte cell line. VEGF mRNA was expressed even in the preadipocyte condition, and its expression was enhanced after adipocyte conversion. Especially, the expression levels of VEGF mRNA were significantly increased 14 days after differentiation. Furthermore, the levels of VEGF protein secretion were almost the same level as gene expression. These results suggest that VEGF production may be dependent on the lipid accumulation (maturation) as well as the time lapse after adipocyte conversion rather than adipocyte differentiation from preadipocytes in 3T3-L1 cells.

We next determined whether VEGF protein secreted from 3T3-L1 cells has some biological activities. To know the role of VEGF in physiological or pathological conditions, we examined the effect of conditioned medium derived from 3T3-L1 cells on in vitro tube formation activity in HUVECs. The conditioned media from pre- and postdifferentiated 3T3-L1 cells enhanced angiogenesis in vascular endothelial cells. These results suggest that VEGF protein secreted from adipocytes may play some roles in the pathological neovascularization observed in diabetic retinopathy or atherosclerosis.

In the third set of experiments, the effects of anatomic localization on fat accumulation and VEGF production in adipocytes were analyzed using a cell implantation technique. 3T3-L1 cells implanted into the mesenteric area of athymic mice expressed more VEGF mRNA than that implanted into the subcutaneous area. The expression of PPARγ was also higher in 3T3-L1 cells implanted into the mesenteric area than into the subcutaneous area, and plasma VEGF concentrations in the mice implanted with 3T3-L1 cells into the mesenteric area were higher than in the subcutaneous area. These results suggest that a certain mechanism may exist in the visceral fat area to make implanted 3T3-L1 cells for enhanced VEGF production.

In summary, these results from in vitro and in vivo experiments indicate that VEGF expression in adipocytes is possibly differentiation as well as time (age) dependent after adipocyte conversion and may be determined by the site of body distribution. Further experiments are required to clarify the mechanism of enhanced expression of VEGF in visceral fat.

GRANTS

These studies were supported by grants from the Japanese Ministry of Education, Science, Sports and Culture.

REFERENCES

1. **Afuwape AO, Kiriakidis S, and Paleolog EM.** The role of the angiogenic molecule VEGF in the pathogenesis of rheumatoid arthritis. *Histol Histopathol* 17: 961–972, 2002.
2. **Aiello LP, Avery RL, Arrigg PG, Keyt BA, Jampel HD, Shah ST, Pasquale LR, Thieme H, Iwamoto MA, Park JE, Nguyen HV, Aiello LM, Ferrara N, and King GL.** Vascular endothelial growth factor in ocular fluid of patients with diabetic retinopathy and other retinal disorders. *N Engl J Med* 331: 1480–1487, 1994.
3. **Chiarelli F, Spagnolit A, Basciani F, Tumini S, Mezzetti A, Cipollone F, Cuccurullo F, Morgese G, and Verrotti A.** Vascular endothelial growth factor (VEGF) in children, adolescents and young adults with Type 1 diabetes mellitus: relation to glycaemic control and microvascular complications. *Diabet Med* 17: 650–656, 2000.
4. **Claffey KP, Wilkison WO, and Spiegelman BM.** Vascular endothelial growth factor. Regulation by cell differentiation and activated second messenger pathways. *J Biol Chem* 267: 16317–16322, 1992.
5. **Dvorak HF, Brown LF, Detmar M, and Dvorak AM.** Vascular permeability factor/vascular endothelial growth factor, microvascular hyperpermeability, and angiogenesis. *Am J Pathol* 146: 1029–1039, 1995.
6. **Ferrara N.** Role of vascular endothelial growth factor in physiologic and pathologic angiogenesis: therapeutic implications. *Semin Oncol* 6: 10–14, 2002.
7. **Hotamisligil GS, Arner P, Caro JF, Atkinson RL, and Spiegelman BM.** Increased adipose tissue expression of tumor necrosis factor-α in human obesity and insulin resistance. *J Clin Invest* 95: 2409–2415, 1995.
8. **Kubota Y, Kleinman HK, Martin GR, and Lawley TJ.** Role of laminin and basement membrane in the morphological differentiation of human endothelial cells into capillary-like structures. *J Cell Biol* 107: 1589–1598, 1988.
9. **Leung DW, Cachianes G, Kuang WJ, Goeddel DV, and Ferrara N.** Vascular endothelial growth factor is a secreted angiogenic mitogen. *Science* 246: 1306–1309, 1989.
10. **MacDougald OA, Hwang CS, Fan H, and Lane MD.** Regulated expression of the obese gene product (leptin) in white adipose tissue and 3T3-L1 adipocytes. *Proc Natl Acad Sci USA* 92: 9034–9037, 1995.
11. **Madrup S, Loftus TM, MacDougald OA, Kuhajda FP, and Lane MD.** Obese gene expression at in vivo levels by fat pads derived from s.c. implanted 3T3-F442A preadipocytes. *Proc Natl Acad Sci USA* 94: 4300–4305, 1997.
12. **Maeda K, Okubo K, Shimomura I, Mizuno K, Matsuzawa Y, and Matsubara K.** Analysis of an expression profile of genes in the human adipose tissue. *Gene* 190: 227–235, 1997.
13. **Matsumoto F, Bujo H, Kuramochi D, Saito K, Shibasaki M, Takahashi K, Yoshimoto S, Ichinose M, and Saito Y.** Effects of nutrition on the cell survival and gene expression of transplanted fat tissues in mice. *Biochem Biophys Res Commun* 295: 630–635, 2002.
14. **Mertens I, Van der Planken M, Corthouts B, Wauters M, Peiffer F, De Leeuw I, and Van Gaal L.** Visceral fat is a determinant of PAI-1 activity in diabetic and non-diabetic overweight and obese women. *Horm Metab Res* 33: 602–607, 2001.
15. **Miyazawa-Hoshimoto S, Takahashi K, Bujo H, Hashimoto N, and Saito Y.** Elevated serum vascular endothelial growth factor is associated with visceral fat accumulation in human obese subjects. *Diabetologia* 46: 1483–1488, 2003.
16. **Paleolog EM.** Angiogenesis in rheumatoid arthritis. *Arthritis Res* 4: S81–S90, 2002.
17. **Ross JS, Stagliano NE, Donovan MJ, Breitbart RE, and Ginsburg GS.** Atherosclerosis: a cancer of the blood vessels? *Am J Clin Pathol* 116: S97–S107, 2001.
18. **Senger DR, Van de Water L, Brown LF, Nagy JA, Yeo KT, Yeo TK, Berse B, Jackman RW, Dvorak AM, and Dvorak HF.** Vascular permeability factor (VPF, VEGF) in tumor biology. *Cancer Metastasis Rev* 12: 303–324, 1993.
19. **Shibasaki M, Takahashi K, Itou T, Miyazawa S, Ito M, Kobayashi J, Bujo H, and Saito Y.** Alterations of insulin sensitivity by the implantation of 3T3-L1 cells in nude mice. A role for TNF-alpha? *Diabetologia* 45: 518–526, 2002.
20. **Shimomura I, Funahashi T, Takahashi M, Maeda K, Kotani K, Nakamura T, Yamashita S, Miura M, Fukuda Y, Takemura K, Tokunaga K, and Matsuzawa Y.** Enhanced expression of PAI-1 in visceral fat: possible contributor to vascular disease in obesity. *Nat Med* 2: 800–803, 1996.
21. **Tsigos C, Kyrou I, Chala E, Tsapogas P, Stavridis JC, Raptis SA, and Katsilambros N.** Circulating tumor necrosis factor alpha concentrations are higher in abdominal versus peripheral obesity. *Metabolism* 48: 1332–1335, 1999.
22. **Vozarova B, Weyer C, Hanson K, Tataranni PA, Bogardus C, and Pratley RE.** Circulating interleukin-6 in relation to adiposity, insulin action, and insulin secretion. *Obes Res* 9: 414–417, 2001.

Clinical Chemistry 51:3
578–585 (2005)

Lipids, Lipoproteins, and Cardiovascular Risk Factors

Adiponectin and other Adipocytokines as Predictors of Markers of Triglyceride-Rich Lipoprotein Metabolism

DICK C. CHAN,[1] GERALD F. WATTS,[1*] THEODORE W.K. NG,[1] YOSHIAKI UCHIDA,[2] NAOHIKO SAKAI,[3] SHIZUYA YAMASHITA,[3] and P. HUGH R. BARRETT[1]

Background: **Adipocytokines are bioactive peptides that may play an important role in the regulation of glucose and lipid metabolism. In this study, we investigated the association of plasma adipocytokine concentrations with markers of triglyceride-rich lipoprotein (TRL) metabolism in men.**

Methods: **Fasting adiponectin, leptin, resistin, interleukin-6 (IL-6), tumor necrosis factor-α (TNF-α), apolipoprotein (apo) B-48, apo C-III, and remnant-like particle (RLP)-cholesterol concentrations were measured by immunoassays and insulin resistance by homeostasis assessment (HOMA) score in 41 nondiabetic men with a body mass index of 22–35 kg/m^2. Visceral and subcutaneous adipose tissue masses (ATMs) were determined by magnetic resonance imaging and total ATM by bioelectrical impedance.**

Results: **In univariate regression, plasma adiponectin and leptin concentrations were inversely and directly associated with plasma apoB-48, apoC-III, RLP-cholesterol, triglycerides, VLDL-apoB, and VLDL-triglycerides (P <0.05). Resistin, IL-6, and TNF-α were not significantly associated with any of these variables, except for a direct correction between apoC-III and IL-6 (P <0.05). In multivariate regression including HOMA, age, nonesterified fatty acids, and adipose tissue compartment, adiponectin was an independent predictor of plasma apoB-48 (β coefficient = −0.354; P = 0.048), apoC-III (β coefficient = −0.406; P = 0.012), RLP-cholesterol (β coefficient = −0.377; P = 0.016), and triglycerides (β coefficient = −0.374; P = 0.013). By contrast, leptin was not an independent predictor of these TRL markers. Plasma apoB-48, apoC-III, RLP-cholesterol, and triglycerides were all significantly and positively associated with plasma insulin, HOMA, and visceral, subcutaneous, and total ATMs (P <0.05).**

Conclusions: **These data suggest that the plasma adiponectin concentration may not only link abdominal fat, insulin resistance, and dyslipidemia, but may also exert an independent role in regulating TRL metabolism.**

Obesity is strongly associated with insulin resistance and dyslipidemia and increased risk of cardiovascular disease (CVD)[4] *(1, 2)*. Hypertriglyceridemia attributable to increased plasma concentrations of VLDL apolipoprotein (apo) B-100 and chylomicron apoB-48 is the most consistent lipid disorder in obesity *(3, 4)*. The precise underlying mechanism for this lipid abnormality remains unclear but may relate to oversecretion, reduced hydrolysis, and/or impaired clearance of triglyceride-rich lipoproteins (TRLs) *(3, 5)*. We have previously shown that obesity in men is associated with increased hepatic secretion and delayed catabolism of TRLs and that these kinetic defects are in part related to accumulation of abdominal fat and insulin resistance *(3, 5)*. We also demonstrated

[1] School of Medicine and Pharmacology, Western Australian Institute for Medical Research, University of Western Australia, Perth, Western Australia, Australia.

[2] Fujirebio Inc., Research and Development Division, Tokyo, Japan.

[3] Department of Internal Medicine and Molecular Science, Osaka University Graduate School of Medicine, Osaka, Japan.

*Address correspondence to this author at: School of Medicine and Pharmacology, University of Western Australia, Royal Perth Hospital, GPO Box X2213, Perth Western Australia 6847, Australia. Fax 61-8-9224-0246; e-mail gfwatts@cyllene.uwa.edu.au.

Received November 6, 2004; accepted December 27, 2004.

Previously published online at DOI: 10.1373/clinchem.2004.045120

[4] Nonstandard abbreviations: CVD, cardiovascular disease; apo, apolipoprotein; TRL, triglyceride-rich lipoprotein; RLP, remnant-like particle; IL-6, interleukin-6; TNF-α, tumor necrosis factor-α; MRI, magnetic resonance imaging; HOMA, homeostasis assessment; BMI, body mass index; ATM, adipose tissue mass; FFM, fat-free mass; SAATM, subcutaneous abdominal adipose tissue mass; IPATM, intraperitoneal adipose tissue mass; RPATM, retroperitoneal adipose tissue mass; NEFA, nonesterified fatty acid; and SDS-PAGE, sodium dodecyl sulfate–polyacrylamide gel electrophoresis.

that obese individuals have insulin resistance and increased concentrations of markers of TRL metabolism, including apoB-48, apoC-III, remnant-like particle (RLP)-cholesterol, non-HDL cholesterol, and triglycerides *(3)*.

The precise relationships between dyslipoproteinemia, adiposity, and insulin resistance are complex and undefined *(2, 4, 6)*. Adipose tissue has recently been shown to secrete a variety of bioactive peptides, called adipocytokines, that can potentially impact on glucose and lipid metabolism *(7–9)*. These adipocytokines include adiponectin, leptin, resistin, interleukin-6 (IL-6), and tumor necrosis factor-α (TNF-α). Adiponectin, also known as adipocyte complement-related protein of 30 kDa (ACRP30), adipoQ, and gelatin-binding protein of 28 kDa (GBP28), is a protein present at relatively high concentrations in the circulation *(9)*. Unlike other adipocytokines, plasma adiponectin concentrations are decreased in obese and insulin-resistant individuals, including those with type 2 diabetes *(10, 11)*. Experimental and clinical evidence suggests that other adipocytokines may exert their effects on insulin sensitivity by influencing adipocyte expression and secretion of adiponectin *(12)*. Hypertriglyceridemia, low HDL-cholesterol concentrations, and decreased LDL particle size have recently been shown in humans to be correlated with low plasma adiponectin concentrations independent of the amount of intraabdominal fat and degree of insulin resistance *(13, 14)*. Moreover, a recent intervention trial reported that changes in adiponectin concentrations after weight loss are correlated with improvements in plasma lipid concentrations independent of changes in adiposity and insulin sensitivity *(13)*. However, the association between plasma adiponectin and specific markers of TRLs in relation to insulin resistance and body fat distribution has not been investigated previously.

In the present study, we hypothesized that, in men, adiponectin would be the adipocytokine most closely associated with changes in TRLs, namely apoB-48 and RLP-cholesterol, and that this association would be independent of body fat compartments and insulin resistance. Our principal aims were (*a*) to examine the association of markers of TRL metabolism, as reflected by plasma concentrations of apoB-48, apoC-III, and RLP-cholesterol, with plasma adiponectin, leptin, resistin, TNF-α, and IL-6 concentrations; and (*b*) to explain these associations in relation to variations in body fat compartments and insulin resistance, measured by magnetic resonance imaging (MRI) and homeostasis assessment (HOMA) score, respectively.

Materials and Methods

STUDY POPULATION

We studied 41 Caucasian men with a body mass index (BMI) ranging from 22 to 35 kg/m^2 and no history of familial dyslipidemia, intercurrent illness, or use of medications affecting lipid metabolism. All were nonsmokers and were consuming ad libitum weight-maintenance diets, as described previously *(15)*. Participants were selected from the community. The study was approved by the Royal Perth Hospital Ethics Committee.

CLINICAL PROTOCOLS

Clinical tests. Body weight, height, and waist and hip circumference were recorded as described previously *(15)*; BMI and waist-to-hip ratio were calculated. Blood pressure was recorded semiautomatically by use of a Dinamap recorder (Critilzon). Body composition was estimated, with participants at rest in the supine position after emptying their bladders, by use of a Holtain Body Composition Analyser (Holtain Ltd.) from which total adipose tissue mass (ATM), fat mass, and fat-free mass (FFM) were derived; FFM was calculated by use of the formula of Lukaski et al. *(16)*: FFM = $(0.85 \times H^2/Z) + 3.04$, where H is the height (cm) of the individual and Z is impedance. For this measure, participants were also asked to refrain from alcoholic beverages for 24 h; they were then studied in the morning, 15 min after emptying their bladder and in a temperature-controlled room. The technical error for FFM was <3%.

Dietary and energy expenditure records. Participants completed a 7-day food intake diary that recorded all dietary, alcohol, and energy intake; data were analyzed by use of DIET4 Nutrient Calculation Software (Xyris Software) based on the Australian Food Composition Database (NUTTAB 95; Australian Government Nutrient Database).

MRI. MRI of eight transaxial segments (field of view, 40–48 cm; 10-mm thickness) at intervertebral disc positions from T11 to S1 was carried out with a 1.0-Tesla Picker MR scanner (Picker International) and a T1-weighted fast-spin-echo sequence with a high fat-to-water signal ratio. Subcutaneous abdominal ATM (SAATM), intraperitoneal ATM (IPATM), and retroperitoneal ATM (RPATM) areas were calculated by summing the relevant adipose tissue pixel units with purpose-designed software, as used previously *(15)*. Fat anterior to the posterior peritoneum and anterior abdominal wall was defined as IPATM, and fat posterior to the posterior peritoneum was defined as RPATM. Anterior and posterior subcutaneous abdominal compartments was separated by drawing a perpendicular line at the midpoint of the anterior–posterior line passing through midpoints of the vertebral bodies in the MRI images. Anterior SAATM was obtained by subtracting posterior SAATM from total SAATM. The imaging protocol has a technical error of <10% and is highly correlated (R^2 = 99%) with measurements obtained from imaging of the abdominal region by contiguous transaxial slices. On the basis of phantom studies using oil/water emulsions, the accuracy of our method for delineating regional adipose tissue was 100.1 (0.01)%. The reproducibility of duplicate in vivo measures of

IPATM and SAATM had a CV <3.5%. Further details are described elsewhere *(15)*.

BIOCHEMICAL ANALYSES

Fasting plasma cholesterol, triglycerides, and HDL-cholesterol were determined by standard enzymatic methods (interassay CVs <3%). LDL-cholesterol was calculated by use of the Friedewald equation. Non-HDL cholesterol was derived as total cholesterol minus HDL-cholesterol. The VLDL fraction was isolated from 3 mL of plasma by ultracentrifugation (Kontron Instruments) at 147 000*g* for 16 h at 4 °C, and the triglyceride concentration was measured as described above. VLDL-apoB concentrations were determined by a modified Lowry method (interassay CV <5%) *(5)*. Plasma nonesterified fatty acids (NEFAs) and glucose were measured by enzymatic methods and insulin by an immunosorbent assay. Insulin resistance was estimated by the HOMA score *(17)*. Plasma apoB-48 concentrations were measured by a sandwich ELISA using anti-human apoB-48 monoclonal antibodies (designated B-48-151) as reported previously (interassay CV <5%) *(18)*. This direct ELISA measurement of apoB-48 in plasma was highly correlated with the traditional method using sodium dodecyl sulfate–polyacrylamide gel electrophoresis (SDS-PAGE) coupled with immunoblotting and enhanced chemiluminescence in frozen plasma samples ($n = 30$; $r = 0.805$; $P < 0.001$) with a wide range of triglyceride concentrations (0.4–5.0 mmol/L) *(19)*. Values were 0.3–17.7 mg/L [mean (SD), 5.5 (4.8) mg/L] for the ELISA method and 9.51–54.40 mg/L [52.3 (11.6) mg/L] for the SDS-PAGE method. Plasma apoC-III was measured by immunoturbidimetric assay (Daiichi). Plasma RLP-cholesterol was determined with a JIMRO-II (Japan Immunoresearch Laboratories) assay using an immunoseparation technique (interassay CV <5%) *(20)*. Plasma adiponectin, leptin, IL-6, TNF-α, and resistin concentrations were measured by enzyme immunoassays (R & D Systems and Phoenix Pharmaceuticals); the interassay CV for these methods were <7%.

STATISTICAL ANALYSES

All analyses were performed with SPSS 11.5 (SPSS). The data are reported as the mean (SD). Skewed data were log-transformed where appropriate. Associations were examined by simple and stepwise linear regression methods. Because we carried out multiple comparisons, we considered that only $P < 0.01$ was of major importance in univariate analysis, but we also considered the conventional $P < 0.05$ as being statistically significant. Multiple regression models were used to determine the variables that best predicted plasma apoB-48, apoC-III, RLP-cholesterol, triglyceride, and VLDL-apoB concentrations. The adipose tissue compartment the most significantly correlated with corresponding dependent variable in stepwise regression analysis was included in the regression models.

Table 1. Anthropometric and ATM characteristics of the 41 men studied.

Characteristics	Mean (SD)	Range
Age, years	47 (9)	25–61
Systolic blood pressure, mmHg	127 (16)	96–164
Diastolic blood pressure, mmHg	76 (10)	53–96
Weight, kg	97 (12)	67–117
BMI, kg/m^2	30 (3)	22–35
Waist-to-hip ratio	1.0 (0.1)	0.9–1.1
FFM, kg	63 (8)	40–83
IPATM, kg	3.7 (1.5)	1.2–8.3
RPATM, kg	0.5 (0.06)	0.1–3.7
SAATM, kg	4.0 (1.4)	1.4–6.9
Anterior SAATM, kg	1.4 (0.6)	0.2–2.9
Posterior SAATM, kg	2.6 (0.9)	0.8–4.4
Total ATM, kg	33 (10)	13–56

Results

The anthropometric and ATM characteristics of the 41 men are shown in Table 1. They were generally middle aged and normotensive. Thirteen were nonobese, and 28 were obese, defined as BMI ≥30 kg/m^2. The mean proportions of total adipose tissue as IPATM, RPATM, and SAATM were 11%, 1.5%, and 12.1%, respectively. Of total SAATM, 35% was in the anterior and 65% in the posterior compartment.

The biochemical characteristics in the individuals studied are shown in Table 2. On average, the group was dyslipidemic, with increased triglycerides and low HDL-cholesterol, and insulin resistant. Four had impaired fasting glucose (6.1–6.9 mmol/L). Mean (SD) dietary intake per day was as follows: energy, 9276 (2030) kJ; total fat, 36 (7)%; carbohydrates, 38 (8)%; protein, 21 (4)%; alco-

Table 2. Biochemical characteristics of the men studied.

Characteristics	Mean (SD)	Range
Cholesterol, mmol/L	5.7 (0.9)	3.8–8.3
Triglycerides, mmol/L	2.7 (1.9)	0.5–8.8
HDL-cholesterol, mmol/L	1.0 (0.3)	0.6–1.8
Non-HDL cholesterol, mmol/L	4.7 (1.0)	3.1–7.4
LDL-cholesterol, mmol/L	3.6 (0.9)	1.5–5.8
RLP-cholesterol, mg/L	367 (34)	52–1670
ApoB-48, mg/L	8.9 (6.1)	1.0–24
ApoC-III, mg/L	163 (98)	29–410
VLDL-triglycerides, mmol/L	1.3 (1.3)	0.1–6.1
VLDL-apoB, mg/L	194 (167)	34–865
VLDL-triglycerides/apoB	13.2 (9.3)	0.36–63.9
NEFAs, mmol/L	0.90 (0.27)	0.45–1.67
Glucose, mmol/L	5.4 (0.6)	4.1–6.9
Insulin, mIU/L	11.7 (8.5)	2.6–41.8
HOMA score	2.9 (2.3)	0.6–10.8
Adiponectin, mg/L	4.4 (2.4)	1.4–11.4
Leptin, μg/L	18 (4)	10–23
Resistin, μg/L	204 (69)	53–366
TNF-α, ng/L	17 (7)	6–39
IL-6, ng/L	12 (5)	4–30

hol, 6 (6)%; and cholesterol, 385 (176) g. Compared with the 13 nonobese men, the 28 obese men had significantly increased plasma glucose, insulin, triglyceride, apoB-48, apoC-III, RLP-cholesterol, non-HDL cholesterol, VLDL-apoB, VLDL-triglycerides, and leptin concentrations and HOMA scores ($P < 0.01$), and significantly lower plasma HDL-cholesterol and adiponectin concentrations ($P < 0.01$), with no significant group differences in plasma resistin, IL-6, or TNF-α concentrations.

The univariate associations of plasma lipid and lipoprotein concentrations with plasma adipocytokine concentrations, measures of insulin resistance, and adipose tissue compartments are shown in Table 3. Plasma adiponectin concentration was significantly and negatively correlated with plasma apoB-48, apoC-III, RLP-cholesterol, triglyceride, total cholesterol, non-HDL cholesterol, VLDL-apoB, and VLDL-triglyceride concentrations and positively with HDL-cholesterol ($P < 0.05$ for both). By contrast, plasma leptin concentration was positively associated with plasma apoB-48, apoC-III, RLP-cholesterol, triglyceride, non-HDL cholesterol, VLDL-apoB, and VLDL-triglyceride concentrations and inversely with HDL-cholesterol (both $P < 0.05$). Plasma VLDL-apoB concentration was significantly and positively correlated with triglyceride ($r = 0.799$; $P < 0.001$), cholesterol ($r = 0.447$; $P < 0.01$), and non-HDL cholesterol ($r = 0.534$; $P < 0.001$) concentrations and negatively with HDL-cholesterol ($r = 0.402$; $P < 0.01$) concentration. The associations of apoB-48, apoC-III, RLP-cholesterol, and triglycerides with plasma adiponectin and leptin are shown in Figs. 1 and 2, respectively. Plasma resistin, IL-6, and TNF-α concentrations were not significantly associated with any of these lipid and lipoprotein variables except for a direct correlation between apoC-III and IL-6 ($r = 0.321$; $P < 0.05$). Plasma apoB-48, apoC-III, RLP-cholesterol, triglyceride, VLDL-apoB, and VLDL-triglyceride concentrations were positively associated with insulin, HOMA score, and the masses of all adipose tissue compartments except for total ATM in the case of VLDL-triglycerides. Plasma apoB-48 concentrations were also highly significant associated (both $P < 0.01$) with plasma concentrations of triglycerides ($r = 0.826$), RLP-cholesterol ($r = 0.732$), non-HDL cholesterol ($r = 0.517$), and VLDL-apoB ($r = 0.829$). Moreover, plasma adiponectin and leptin concentrations were significantly associated with insulin concentrations, HOMA score, and the masses of all adipose tissue compartments except for RPATM. Plasma resistin, IL-6, and TNF-α were not significantly associated with insulin concentration, HOMA score, and the masses of all adipose tissue compartments except for IPATM in the case of IL-6 and TNF-α (data not shown).

As shown in Table 4, plasma adiponectin concentration was a significant independent predictor of plasma apoB-48, apoC-III, RLP-cholesterol, and triglyceride concentrations ($P < 0.05$) in regression models including HOMA score, adipose tissue compartment, age, and NEFAs. Plasma adiponectin concentration was also a significant independent predictor of plasma VLDL-apoB (β coefficient = -0.377; $P = 0.016$) and VLDL-triglyceride (β coefficient = -0.364; $P = 0.042$) concentrations. In these models, IPATM was also an independent predictor of plasma apoC-III and VLDL-apoB concentrations, whereas total SAATM was an independent predictor of plasma triglyceride concentrations (Table 4). In contrast to adiponectin, plasma leptin was not an independent predictor of plasma apoB-48, apoC-III, RLP-cholesterol, and triglyceride concentrations in the same regression models (Table 4). In these models, total SAATM was an independent predictor of plasma apoB-48 and triglyceride concentrations, whereas HOMA score was an indepen-

Table 3. Associations (Pearson correlation coefficients) of plasma lipid and lipoprotein concentrations with plasma adipocytokine concentrations, measures of insulin resistance, and adipose tissue compartments.

	ApoB-48	ApoC-III	RLP-C[a]	TG	Cholesterol	HDL-C	Non-HDL C	LDL-C	VLDL-apoB	VLDL-TG
Adiponectin	−0.506[b]	−0.531[b]	−0.557[b]	−0.632[b]	−0.453[b]	0.474[b]	−0.564[b]	−0.172	−0.622[b]	−0.452[b]
Leptin	0.342[c]	0.400[b]	0.423[b]	0.548[b]	0.224	−0.414[b]	0.334[c]	0.050	0.463[b]	0.359[c]
Resistin	−0.113	0.027	−0.073	0.034	0.007	0.120	−0.014	−0.009	−0.010	−0.153
TNF-α	0.057	0.204	0.255	0.198	0.197	−0.105	0.227	0.119	0.187	0.197
IL-6	0.067	0.321[c]	0.166	0.169	0.132	−0.060	0.133	0.149	0.167	0.110
NEFAs	−0.207	−0.156	−0.200	−0.197	−0.078	0.163	−0.111	−0.063	−0.167	−0.042
Glucose	0.241	0.364[c]	0.387[c]	0.401[b]	0.016	−0.370[c]	0.108	−0.135	0.367[c]	0.335[c]
Insulin	0.483[b]	0.511[b]	0.613[b]	0.660[b]	0.423[b]	−0.439[b]	0.525[b]	0.119	0.572[b]	0.386[c]
HOMA score	0.343[c]	0.411[b]	0.512[b]	0.671[b]	0.395[b]	−0.459[b]	0.509[b]	0.092	0.440[b]	0.319[c]
IPATM	0.440[b]	0.508[b]	0.490[b]	0.565[b]	0.266	−0.366[c]	0.360[c]	0.022	0.553[b]	0.347[c]
RPATM	0.335[c]	0.382[c]	0.398[c]	0.438[b]	0.206	−0.285	0.280	0.025	0.310[c]	0.337[c]
Total SAATM	0.491[b]	0.401[b]	0.435[b]	0.591[b]	0.317[c]	−0.433[b]	0.431[b]	0.132	0.517[b]	0.417[c]
Anterior SAATM	0.458[b]	0.385[c]	0.386[c]	0.546[b]	0.255	−0.340[b]	0.342[c]	0.018	0.452[b]	0.420[c]
Posterior SAATM	0.462[b]	0.369[c]	0.424[b]	0.560[b]	0.328[c]	−0.453[b]	0.450[b]	0.195	0.508[b]	0.371[c]
Total ATM	0.386[c]	0.367[c]	0.396[c]	0.468[b]	0.301	−0.309[c]	0.381[c]	0.173	0.490[b]	0.254

[a] RLP-C, remnant-like particle-cholesterol; TG, triglycerides; HDL-C, HDL-cholesterol; Non-HDL C, non-HDL cholesterol; LDL-C, LDL-cholesterol.
[b,c] Significant at [b]$P < 0.01$; [c]$P < 0.05$.

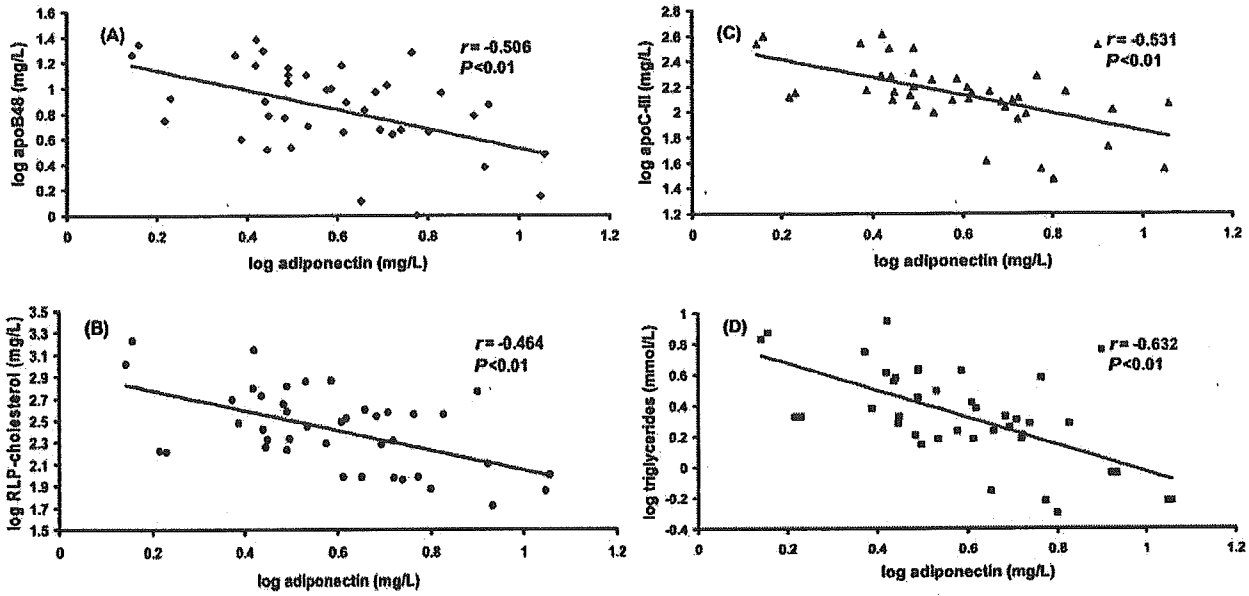

Fig. 1. Associations of plasma adiponectin concentrations with apoB-48 (*A*), apoC-III (*B*), RLP-cholesterol (*C*), and triglyceride (*D*) concentrations.

dent predictor of plasma RLP-cholesterol and triglyceride concentrations. Plasma IL-6 concentration was not an independent predictor of plasma apoC-III in the regression models including HOMA, age, NEFAs, and IPATM (data not shown).

Discussion

We report on the relationships between a wide spectrum of plasma adipocytokines and markers of TRL metabolism in humans. Our principal result was that low plasma adiponectin concentrations were highly predictive of increased plasma apoB-48, apoC-III, RLP-cholesterol, and triglyceride concentrations and that this was independent of both insulin resistance and size of adipose tissue compartments. Another new finding was that, in these men, other adipocytokines (resistin, IL-6, and TNF-α) were not significantly associated with these markers except for a direct association between plasma apoC-III and IL-6 concentrations. In the case of leptin, significant associations were not independent of body fat compartments and insulin resistance. We also showed good agreement across a wide range of plasma triglyceride concentrations

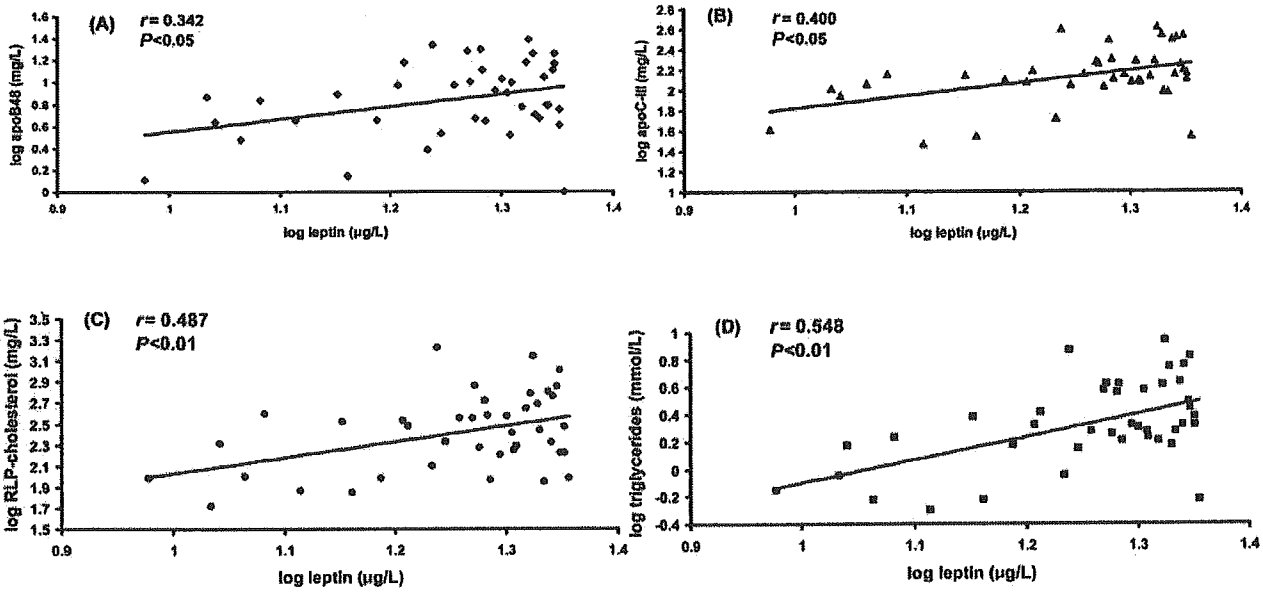

Fig. 2. Associations of plasma leptin concentrations with apoB-48 (*A*), apoC-III (*B*), RLP-cholesterol (*C*), and triglyceride (*D*) concentrations.

Table 4. Multiple regression analyses of the relationships between markers of TRL metabolism, plasma adiponectin or leptin, HOMA, and adipose tissue compartment.[a]

	Predictor	β coefficient	P	Adjusted R^2
ApoB-48	Adiponectin	−0.354	0.044	
	HOMA	0.019	0.909	
	Total SAATM	0.297	0.072	
				28% ($P = 0.005$)
	Leptin	−0.200	0.386	
	HOMA	0.187	0.259	
	Total SAATM	0.576	0.013	
				21% ($P = 0.019$)
ApoC-III	Adiponectin	−0.406	0.012	
	HOMA	0.038	0.820	
	IPATM	0.322	0.047	
				33% ($P = 0.002$)
	Leptin	0.093	0.618	
	HOMA	0.19	0.274	
	IPATM	0.354	0.077	
				20% ($P = 0.025$)
RLP-cholesterol				
	Adiponectin	−0.377	0.016	
	HOMA	0.203	0.219	
	IPATM	0.236	0.130	
				36% ($P = 0.001$)
	Leptin	0.133	0.461	
	HOMA	0.336	0.049	
	IPATM	0.241	0.207	
				26% ($P = 0.008$)
Triglycerides				
	Adiponectin	−0.374	0.013	
	HOMA	0.213	0.129	
	Total SAATM	0.325	0.021	
				49% ($P = 0.001$)
	Leptin	0.099	0.623	
	HOMA	0.335	0.024	
	Total SAATM	0.403	0.044	
				40% ($P = 0.001$)

[a] The adipose tissue compartment most closely correlated with the corresponding dependent variable in stepwise regression analysis was included in the models, and statistical models were also adjusted for age and NEFAs.

between a new direct ELISA for apoB-48 and a previously published method based on SDS-PAGE coupled with immunoblotting and enhanced chemiluminescence *(19)*.

Our data are consistent with previous findings that low adiponectin concentrations are associated with an atherogenic lipid profile, including increased triglycerides and low HDL-cholesterol *(13, 14, 21)*. We have extended these studies by investigating the association of plasma adiponectin concentrations with markers of TRL metabolism as measured by plasma apoB-48, apoC-III, and RLP-cholesterol concentrations and demonstrating that low adiponectin concentrations are most closely correlated with accumulation of TRLs independent of insulin resistance and body fat distribution. We also provide new data, based on comprehensive investigation of body fat compartments by MRI, that plasma concentrations of apoB-48, apoC-III, and RLP-cholesterol are strongly associated with adipose tissue compartments, including IPATM, RPATM, anterior SAATM, posterior SAATM, and total ATM.

Dyslipidemia in obesity and insulin resistance is fundamentally related to expansion in the plasma pool of TRLs *(6, 22)*. Accumulation of adipose fat, particularly in the abdominal region, leads to a markedly increased flux of NEFAs to the liver *(6, 23)*, which stimulates triglyceride synthesis *(24)*. Insulin resistance increases hepatic synthesis of lipid substrates and the secretion of VLDL apoB-100; it also down-regulates LDL receptors *(22, 25)*. These effects potentially increase the plasma concentrations of remnant lipoproteins containing apoB-100 and increase competition for hepatic uptake between chylomicron and VLDL remnants *(26)*. However, the lack of a significant correlation of plasma NEFAs with VLDL-triglyceride and/or total triglyceride concentration in our study suggests that measurement of circulating NEFAs in plasma may not simply reflect portal flow of NEFAs to the liver. We have previously reported that, in obese men, accumulation of TRL remnants is attributable to defective lipolysis and impaired clearance of chylomicron remnants, as reflected by increased apoC-III concentrations and a reduced catabolic rate of a remnant-like emulsion *(3)*. The metabolic differences between obese and nonobese men in this study were consistent with our previous data *(3)*. We also demonstrated that insulin resistance and body fat distribution were strongly and independently predictive of plasma apoB-48, apoC-III, RLP-cholesterol, triglyceride, and VLDL-apoB concentrations.

The effect of adiponectin on TRL metabolism may principally involve intrinsic changes in skeletal muscle lipid metabolism and effects on lipoprotein lipase activity in both skeletal muscle and adipocytes *(8, 27, 28)*. Adiponectin may decrease accumulation of triglycerides in skeletal muscle by enhancing fatty acid oxidation through activation of acetyl-CoA oxidase, carnitine palmitoyltransferase-1, and AMP kinase *(27)*. Adiponectin may also stimulate both lipoprotein lipase *(29)*, the lipolytic enzyme that catabolizes VLDL, and apoC-III by increasing the expression of peroxisome proliferator-activated receptor-α in the liver and adipocytes *(30)*. At the hepatic level, adiponectin may decrease the supply of NEFAs to the liver for gluconeogenesis, hence decreasing triglyceride synthesis. Taken together, low circulating adiponectin concentrations could lead to delayed removal of TRLs by the liver and peripheral tissue by increasing competition between chylomicrons and VLDL for LPL lipolysis, and between chylomicron remnants and VLDL remnants for LDL-receptor-mediated clearance *(26)*. Because resistin, IL-6, and TNF-α were not associated with insulin resistance and total body fat in the present study, it was not surprising that we found no significant association of these peptides with markers of TRLs. Our findings also suggest that plasma leptin may not per se have a direct

impact on the metabolism of TRLs and may simply reflect changes in body fat stores *(31)*.

Several methods have been used for the measurement of apoB-48 in plasma *(18, 19, 32)*. The Western blotting method is time-consuming and is less quantitative than the standard ELISA technique; the specificity of polyclonal antibodies in the competitive ELISA is also questionable. In the present study, we used a novel ELISA system that incorporates monoclonal antibodies against apoB-48 to measure apoB-48 in plasma *(18)*. This method enhances the specificity and sensitivity of apoB-48 measurements in plasma without the need for time-consuming isolation of TRLs. Differences in fasting apoB-48 values reported by different methods reflect differences in standardization *(32)*. Despite the analytical shortcomings listed above, we found that the apoB-48 values obtained by our ELISA and the SDS-PAGE methods were well correlated.

We used a surrogate estimate of insulin resistance, the HOMA score, which is well correlated with the hyperinsulinemic, euglycemic clamp technique *(17)*. Measurements of apoB-48 may not differentiate between the nascent chylomicron and its remnant. However, because participants were fasted for at least 12 h to ensure minimal intestinal secretion of nascent chylomicrons, the apoB-48 concentration was probably indicative of small, dense chylomicrons and their remnants. In addition, fasting RLP-cholesterol is not a specific marker of chylomicron and VLDL remnants because it quantifies apoE-rich lipoproteins of intestinal origin as well as some hepatic lipoproteins *(20, 33)*. The association of plasma adipocytokines with apoC-III kinetics also requires further investigation. Future studies should examine the effect of adiponectin genotypes on TRL metabolism *(34, 35)*. In addition, the individual effects of the full-length peptide as well as the low- and high-molecular-weight forms of adiponectin on TRL metabolism also merit further investigation *(36)*.

Several studies have clearly demonstrated the close relationship between the impaired metabolism of TRLs and the development of CVD and type 2 diabetes *(33, 37–39)*. Clinical and experimental data have also recently demonstrated that adiponectin is a strongly protective predictor of CVD, having several antiatherogenic properties *(28, 40, 41)*. Our study therefore suggests that the relationship between low adiponectin concentrations and CVD may in part be mediated by the accumulation of TRLs in plasma. However, definitive evidence of the role of adiponectin in regulating TRL metabolism will require further investigation using adiponectin-knockout animals and recombinant adiponectin replacement therapy *(29)*.

This work was supported by the National Heart Foundation of Australia, the National Health and Medical Research Council (NHMRC), Raine Foundation, Pfizer Inc., and Glaxo Smith Kline. This work was also supported by a grant from AstraZeneca and Shionogi Pharmaceutical Co. to S.Y. and by grants from Future Research Forum Japan (supported by AstraZeneca and Shionogi & Co., Ltd.) to S.Y. and N.S. P.H.R.B. is a Senior Research Fellow of NHMRC and was also supported by the National Institutes of Health (NIBIB P41 EB-001975). We also thank Associate Professor John C.L. Mamo and Dr. Anthony P. James for apoB-48 measurements by immunoblotting (Curtin University of Technology, Western Australia). D.C.C. was supported by a postdoctoral fellowship from the Raine-National Heart Foundation of Australia.

References

1. Després J-P, Moorjani S, Lupien PJ, Tremblay A, Nadeau A, Bouchard C. Regional distribution of body fat, plasma lipoproteins and cardiovascular disease. Arterioscler Thromb Vasc Biol 1990; 10:497–511.
2. Grundy SM. Obesity, metabolic syndrome, and cardiovascular disease. J Clin Endocrinol Metab 2004;89:2595–600.
3. Chan DC, Watts GF, Barrett PHR, Mamo JCL, Redgrave TG. Markers of triglyceride-rich lipoprotein remnant metabolism in visceral obesity. Clin Chem 2002;48:278–83.
4. Chan DC, Barrett PHR, Watts GF. Dyslipidemia in visceral obesity: mechanisms, implications, and therapy. Am J Cardiovasc Drugs 2004;4:227–46.
5. Riches FM, Watts GF, Naoumova RP, Kelly JM, Croft KD, Thompson GR. Hepatic secretion of very-low-density lipoprotein apolipoprotein B-100 studied with a stable isotope technique in men with visceral obesity. Int J Obes Relat Metab Disord 1998;22: 414–23.
6. Despres JP. Dyslipidaemia and obesity. Baillieres Clin Endocrinol Metab 1994;8:629–60.
7. Meier U, Gressner AM. Endocrine regulation of energy metabolism: review of pathobiochemical and clinical chemical aspects of leptin, ghrelin, adiponectin, and resistin. Clin Chem 2004;50: 1511–25.
8. Havel PJ. Update on adipocyte hormones: regulation of energy balance and carbohydrate/lipid metabolism. Diabetes 2004;53: 143–51.
9. Berg AH, Combs TP, Scherer PE. ACRP30/adiponectin: an adipokine regulating glucose and lipid metabolism. Trends Endocrinol Metab 2002;13:84–9.
10. Arita Y, Kihara S, Ouchi N, Takahashi M, Maeda K, Miyagawa J, et al. Paradoxical decrease of an adipose-specific protein, adiponectin, in obesity. Biochem Biophys Res Commun 1999;257:79–83.
11. Hotta K, Funahashi T, Arita Y, Takahashi M, Matsuda M, Okamoto Y. Plasma concentrations of a novel, adipose-specific protein, adiponectin, in type 2 diabetic patients. Arterioscler Thromb Vasc Biol 2000;20:1595–9.
12. Bruun JM, Lihn AS, Verdich C, Pedersen SB, Toubro S, Astrup A, et al. Regulation of adiponectin by adipose tissue-derived cytokines: in vivo and in vitro investigations in humans. Am J Physiol Endocrinol Metab 2003;285:527–33.
13. Baratta R, Amato S, Degano C, Farina MG, Patane G, Vigneri R, et al. Adiponectin relationship with lipid metabolism is independent of body fat mass: evidence from both cross-sectional and intervention studies. J Clin Endocrinol Metab 2004;89:2665–71.
14. Cnop M, Havel PJ, Utzschneider KM, Carr DB, Sinha MK, Boyko EJ, et al. Relationship of adiponectin to body fat distribution, insulin sensitivity and plasma lipoproteins: evidence for independent roles of age and sex. Diabetologia 2003;46:459–69.
15. Chan DC, Watts GF, Sussekov AV, Barrett PH, Yang Z, Hua J, et al. Adipose tissue compartments and insulin resistance in over-

weight-obese Caucasian men. Diabetes Res Clin Pract 2004;63: 77–85.
16. Lukaski HC, Johnson PE, Bolonchuk WW, Lykken GI. Assessment of fat-free mass using bioelectrical impedance measurements of the human body. Am J Clin Nutr 1985;41:810–7.
17. Matthews DR, Hosker JP, Rudenski AS, Naylor BA, Treacher DF, Turner RC. Homeostasis model assessment: insulin resistance and B-cell function from fasting plasma glucose and insulin concentrations in man. Diabetologia 1985;28:412–9.
18. Sakai N, Uchida Y, Ohashi K, Hibuse T, Saika Y, Tomari Y, et al. Measurement of fasting serum apoB-48 levels in normolipidemic and hyperlipidemic subjects by ELISA. J Lipid Res 2003;44: 1256–62.
19. Smith D, Proctor SD, Mamo JCL. A highly sensitive assay for quantitation of apolipoprotein B-48 using an antibody to human apolipoprotein B and enhanced chemiluminescence. Ann Clin Biochem 1997;34:185–9.
20. Nakajima K, Saito T, Tamura A, Suzuki M, Nakano T, Adachi M, et al. Cholesterol in remnant-like lipoproteins in human serum using monoclonal anti apo B-100 and anti apo A-I immunoaffinity mixed gels. Clin Chim Acta 1993;223:53–71.
21. Schulze MB, Rimm EB, Shai I, Rifai N, Hu FB. Relationship between adiponectin and glycemic control, blood lipids, and inflammatory markers in men with type 2 diabetes. Diabetes Care 2004;27:1680–7.
22. Ginsberg HN, Huang LS. The insulin resistance syndrome: impact on lipoprotein metabolism and atherothrombosis. J Cardiovasc Risk 2000;7:325–31.
23. Wajchenberg BL. Subcutaneous and visceral adipose tissue: their relation to the metabolic syndrome. Endocr Rev 2000;21:697–738.
24. Lewis GF. Fatty acid regulation of very low density lipoprotein production. Curr Opin Lipidol 1997;8:146–53.
25. Lewis GF, Steiner G. Acute effects of insulin in the control of VLDL production in humans. Implications for the insulin-resistant state. Diabetes Care 1996;19:390–3.
26. Cooper AD. Hepatic uptake of chylomicron remnants. J Lipid Res 1997;38:2173–92.
27. Yamauchi T, Kamon J, Minokoshi Y, Ito Y, Waki H, Uchida S, et al. Adiponectin stimulates glucose utilization and fatty-acid oxidation by activating AMP-activated protein kinase, Nat Med 2002;8: 1288–95.
28. Chandran M, Phillips SA, Ciaraldi T, Henry RR. Adiponectin: more than just another fat cell hormone? Diabetes Care 2003;26: 2442–50.
29. Combs TP, Pajvani UB, Berg AH, Lin Y, Jelicks LA, Laplante M, et al. A transgenic mouse with a deletion in the collagenous domain of adiponectin displays elevated circulating adiponectin and improved insulin sensitivity. Endocrinology 2004;145:367–83.
30. Yamauchi T, Kamon J, Waki H, Terauchi Y, Kubota N, Hara K, et al. The fat-derived hormone adiponectin reverses insulin resistance associated with both lipoatrophy and obesity. Nat Med 2001;7: 941–6.
31. Unger RH. Weapons of lean body mass destruction: the role of ectopic lipids in the metabolic syndrome. Endocrinology 2003; 144:5159–65.
32. Jackson KG, Williams CM. Apolipoprotein B-48: comparison of fasting concentrations measured in normolipidaemic individuals using SDS-PAGE, immunoblotting and ELISA. Atherosclerosis 2004;176:207–17.
33. Twickler TB, Dallinga-Thie GM, Cohn JS, Chapman MJ. Elevated remnant-like particle cholesterol concentration: a characteristic feature of the atherogenic lipoprotein phenotype. Circulation 2004;109:1918–25.
34. Menzaghi C, Ercolino T, Paola RD, Berg AH, Warram JH, Scherer PE, et al. A haplotype at the adiponectin locus is associated with obesity and other features of the insulin resistance syndrome. Diabetes 2002;51:2306–12.
35. Ohashi K, Ouchi N, Kihara S, Funahashi T, Nakamura T, Sumitsuji S, et al. Adiponectin I164T mutation is associated with the metabolic syndrome and coronary artery disease. J Am Coll Cardiol 2004;43:1195–200.
36. Pajvani UB, Hawkins M, Combs TP, Rajala MW, Doebber T, Berger JP, et al. Complex distribution, not absolute amount of adiponectin, correlates with thiazolidinedione-mediated improvement in insulin sensitivity. J Biol Chem 2004;279:12152–62.
37. Ginsberg HN. New perspectives on atherogenesis: role of abnormal triglyceride-rich lipoprotein metabolism. Circulation 2002; 106:2137–42.
38. Fukushima H, Sugiyama S, Honda O, Koide S, Nakamura S, Sakamoto T, et al. Prognostic value of remnant-like lipoprotein particle levels in patients with coronary artery disease and type II diabetes mellitus. J Am Coll Cardiol 2004;43:2219–24.
39. Patsch JR, Miesenbock G, Hopferwieser T, Muhlberger V, Knapp E, Dunn JK, et al. Relation of triglyceride metabolism and coronary artery disease. studies in the postprandial state. Arterioscler Thromb Vasc Biol 1992;12:1336–45.
40. Pischon T, Girman CJ, Hotamisligil GS, Rifai N, Hu FB, Rimm EB. Plasma adiponectin levels and risk of myocardial infarction in men. JAMA 2004;291:1730–7.
41. Matsuzawa Y, Funahashi T, Kihara S, Shimomura I. Adiponectin and metabolic syndrome. Arterioscler Thromb Vasc Biol 2004;24: 29–33.

Identification of Unique Lipoprotein Subclasses for Visceral Obesity by Component Analysis of Cholesterol Profile in High-Performance Liquid Chromatography

Mitsuyo Okazaki, Shinichi Usui, Masato Ishigami, Naohiko Sakai, Tadashi Nakamura, Yuji Matsuzawa, Shizuya Yamashita

Objective—The contribution of visceral fat accumulation to the development of coronary heart disease was previously reported, but the relation between visceral fat accumulation and serum lipoprotein subclasses was unknown.

Methods and Results—We examined the relation of lipoprotein subclasses with visceral fat accumulation in 62 male subjects (aged 22 to 67 years) with visceral fat syndrome or obesity. Cholesterol levels in very low–density, low-density, and high-density lipoprotein subclasses (VLDL, LDL, and HDL) were determined by computer-assisted high-performance liquid chromatography. Subcutaneous fat area and visceral fat area were measured by computed tomographic scanning. There was no significant correlation between the subcutaneous fat area and the cholesterol levels in all lipoprotein subclasses. In contrast, the visceral fat area was correlated positively ($P<0.002$) with VLDL and LDL subclasses, except for large LDL, but negatively ($P<0.001$) with those in large and medium HDL subclasses. The observed positive correlations of small and very small LDL subclasses remained significant ($P<0.005$) after adjustment for serum cholesterol, triglycerides, HDL cholesterol, and LDL cholesterol, respectively, but a significant negative correlation ($P<0.005$) of large LDL was obtained after adjustment for LDL cholesterol.

Conclusion—These findings indicate that this simple high-performance liquid chromatography method may be applied for easy detection and evaluation of abnormal distribution of lipoprotein subclasses. ***(Arterioscler Thromb Vasc Biol.* 2005; 25:578-584.)**

Key Words: obesity ■ risk factors ■ particle size ■ triglyceride

Lipoprotein profiles are well accepted as predictors of risk for coronary heart disease (CHD). The important relationship between elevated low-density lipoprotein cholesterol (LDL-C) or decreased high-density lipoprotein cholesterol (HDL-C) and the increased risk of CHD is definitely established in many epidemiological studies.[1,2] Another established risk factor for cardiovascular disease is obesity, which was confirmed to be a strong positive predicting factor of CHD in the Framingham Heart Study, and the risk for CHD is particularly increased when abdominal obesity is present.[3] Although measurement of LDL-C and HDL-C has been recommended by the U.S. National Cholesterol Education Program for initial classification of CHD risk status,[4] obesity is not considered to be a major risk factor, because the incremental risk imparted by obesity independently of accompanying risk factors is uncertain. Atherogenic dyslipidemia frequently found in abdominal obesity is a combination of high serum triglycerides (TG) and low HDL-C, which is a strong correlate of the small dense LDL phenotype.[5] Cholesterol synthesis is increased in men with visceral obesity, and this may be partly related to insulin resistance, and the reduction in visceral fat is associated with a decrease in the hepatic secretion of VLDL apolipoprotein B (apoB).[6] We also previously reported that the contribution of visceral fat accumulation to the development of CHD is partially through progression of insulin resistance in nonobese men.[7] The visceral fat area (VFA) had significant positive correlations with serum total cholesterol (TC), serum TG, apoB, and apoE levels and the concentrations of VLDL-C, intermediate density lipoprotein cholesterol (IDL-C), and LDL-C.

Many studies showed that LDL subclasses, characterized by variations in their density, size, and chemical composition, might be clinically significant.[8,9] Although earlier studies for lipoprotein subclass analysis have been done by analytical ultracentrifugation,[10] density analysis by various preparative ultracentrifugation methods have also been used: sequential separation at various density,[11] rate zonal ultracentrifugation,[12] and density gradient ultracentrifugation.[13] The particle

Original received September 19, 2004; final version accepted December 12, 2004.

From the Laboratory of Chemistry (M.O.), College of Liberal Arts and Sciences, Tokyo Medical and Dental University, Ichikawa; Faculty of Health Sciences (S.U.), Okayama University Medical School, Okayama; and the Department of Internal Medicine and Molecular Science (M.I., N.S., T.N., Y.M., S.Y.), Osaka University Graduate School of Medicine, Osaka, Japan.

Correspondence to Prof Mitsuyo Okazaki, PhD, Laboratory of Chemistry, College of Liberal Arts and Sciences, Tokyo Medical and Dental University, 2-8-30, Kohnodai, Ichikawa-shi, Chiba 272-0827, Japan. E-mail okazaki.las@tmd.ac.jp

Arterioscler Thromb Vasc Biol. **is available at http://www.atvbaha.org** **DOI: 10.1161/01.ATV.0000155017.60171.88**

size analysis by nondenaturing gradient gel electrophoresis has been used,[14,15] and recently the Lipoprint LDL system (Quantimetrix) using nongradient (3%) polyacrylamide gel electrophoretic method has been developed.[16] More recently, a rapid and convenient method using nuclear magnetic resonance (NMR) has been developed[17,18] and used widely in clinical subjects.[19,20] Many methods for detection and quantification of LDL subclasses based on their particle size, density, shape, and charge were reported, but it is unclear which method is clinically useful.[21]

High-performance liquid chromatography (HPLC) with gel permeation columns is an alternative method for classifying and quantifying lipoproteins on the basis of differences of particle size.[22,23] We successfully applied this technique to compare the effects of bezafibrate and pravastatin on lipoprotein subclasses in type 2 diabetes.[24] The HPLC method, similar to the NMR, measures all lipoprotein subclasses at a single analysis from very small amount of whole serum or plasma in a very short time. The HPLC, however, may be superior because of direct cholesterol determination available in major lipoproteins and their subclasses.

In this study, a new simple and fully automated method for analyzing lipoprotein subclasses by HPLC with gel permeation columns followed by mathematical treatment on chromatograms was applied to examine the relationship of cholesterol levels in lipoprotein subclasses with visceral fat accumulation in men with obesity or nonobese subjects with accumulation of visceral fat. The clinical significance for measurements of the cholesterol levels in all lipoprotein subclasses by HPLC method will be evaluated on the basis of visceral fat accumulation, which plays an important role in the occurrence of CHD associated with a cluster of multiple risk factors.

Methods

Subjects

Sixty-two men (aged 22 to 67 years) were enrolled in this study, which included 15 healthy volunteers and 47 hospitalized patients in Osaka University Hospital. All of the subjects gave their informed consent before entering the study according to the Osaka University Hospital ethics committees. All patients had no severe hepatic or renal diseases, and none of them had any medication known to affect insulin action or serum lipoprotein levels. Venous blood was drawn after an overnight fasting. Serum samples were kept in a refrigerator and analyzed within 7 days after blood collection.

HPLC Method

Serum lipoproteins were analyzed by HPLC, as previously described.[23,25] In brief, 5 μL whole serum sample was injected into 2 connected columns (300×7.8 mm) of TSKgel LipopropakXL (Tosoh) and eluted by TSKeluent Lp-1 (Tosoh). The effluent from the columns was continuously monitored at 550 nm after an online enzymatic reaction with a commercial kit, Determiner L TC (Kyowa Medex). The cholesterol concentration in major lipoproteins and their subclasses was calculated by our own computer program, which was designed to process the complex chromatograms with the modified Gaussian curve fitting for resolving the overlapping peaks by mathematical treatment.

We determined the number, position, and width of each Gaussian component peak for subclass analysis to carry out a sufficient curve fitting analysis of various samples from animals and humans under the constant condition in which the peak width and position of each Gaussian curve were not changed. For this purpose, we first took priority to refer the mean particle size of VLDL and LDL of healthy normolipidemic men (n=28). Therefore, the positions of component peaks 6 and 9 corresponded to those of VLDL (36.8±2.5 nm) and LDL (25.5±0.4 nm) of healthy subjects, respectively. Similarly, the positions of peaks 5 and 10 were those of VLDL (44.5±2.1 nm) and LDL (23.0±0.5 nm) of extremely hypertriglyceridemic subjects >1000 mg/dL (n=7) with or without lipoprotein lipase (LPL), respectively. Peak 7 corresponded to LDL (or VLDL; 31.3±1.0 nm) of type III hyperlipidemia with apoE2/2 (n=5). Peak 15 was HDL (13.5±0.4 nm) of cholesterol ester transfer protein deficiency (n=6). Other component peaks (peaks 16 to 20) of HDL subclasses were based on the 5 subclasses determined by HPLC using a gel permeation column (G3000SW) with a separation range for only HDL.[23,26] In addition to the 11 component peaks determined by some experimental background as described above, 9 additional peaks (peaks 1 to 4, 8, and 11 to 14) were introduced to obtain the best curve fitting analysis by changing only peak height of each Gaussian curve. The position of peak 8 (28.6 nm) was determined as the middle point between peak 7 and peak 9, representing a transition component from TG-rich remnant lipoproteins to LDL. Four peaks (peaks 11 to 14) were regularly inserted between peak 10 and peak 15 to make similar intervals from peak 8 to peak 20. Moreover, 3 peaks (peaks 2 to 4) at least needed to be introduced between a void volume (peak 1) and peak 5 to perform the best curve fitting. Alternative setting of additional peaks resulted in the decrease of the degree of curve fitting analysis on the original chromatogram. The conversion of elution time to particle diameter was performed using a column calibration curve, a plot of logarithm of the particle diameter of standard samples, latex beads (Magsphere Inc) 25 and 37 nm in diameter, and a high molecular weight calibrator (Pharmacia Biotech) containing thyroglobulin (17 nm), ferritin (12.2 nm), catalase (9.2 nm), albumin (7.1 nm), and ovalbumin (6.1 nm) against their elution times.

Other Clinical and Lipid Parameter Analysis

Serum TC and TG were determined enzymatically using commercial kits (Kyowa Medex). HDL-C was quantified by the heparin-Ca^{2+} precipitation method.[27] LDL-C was calculated from the formula of Friedewald et al.[28] Uric acid (UA), fasting immunoreactive insulin (IRI), and plasminogen activator inhibitor (PAI)-1 were measured by enzymatic methods and by a double antibody radioimmunoassay, respectively.

Body fat distribution was determined by computed tomographic (CT) scanning (General Electric CT/T scanner, General Electric Co) in the supine position as described previously.[29] The fat layer to the

TABLE 1. Clinical Characteristics, Lipid, and Lipoprotein Profiles of 62 Men

	Mean±SD	Min/Max
Age, years	43.8±11.3	22/67
Height, cm	169.8±6.3	152/181
Weight, kg	77.5±15.1	56/135
BMI, kg/m^2	26.8±4.6	21.0/43.1
VFA, cm^2	129.2±50.4	24.0/255.0
SFA, cm^2	195.5±97.9	55.0/512.0
UA, mg/dL	6.4±1.7	3.8/12.5
IRI, μU/mL	9.3±7.7	2.0/42.8
PAI-1, ng/mL	25.4±18.6	5.0/75.7
TC, mg/dL	212.6±35.2	135.0/308.7
TG, mg/dL	146.3±88.3	41.5/416.0
HDL-C, mg/dL*	45.0±12.4	22.6/70.7
LDL-C, mg/dL†	138.3±34.5	61.1/211.5

*Determined by the precipitation method.
†Calculated by the Friedwald equation.

TABLE 2. Definition for Major and Subclasses of Serum Lipoproteins and Within-Day Precision (n=5) for Measurement of Their Cholesterol Levels

Component Peak No.	Particle Diameter (nm)	Major and Subclass Name	Pool 1 (mg/dL)			Pool 2 (mg/dL)		
			Mean	SD	CV%	Mean	SD	CV%
1	>90		NA	NA	NA	3.69	0.04	1.03
2	75		NA	NA	NA	2.06	0.06	3.13
3	64	large VLDL	0.06	0.01	20.69	1.95	0.04	2.30
4	53.6	large VLDL	1.16	0.04	3.07	1.65	0.06	3.86
5	44.5	large VLDL	2.37	0.09	3.76	7.58	0.24	3.14
6	36.8	medium VLDL	9.78	0.12	1.27	16.12	0.29	1.83
7	31.3	small VLDL	7.45	0.31	4.21	12.71	0.23	1.78
8	28.6	large LDL	27.92	0.98	3.51	18.56	0.46	2.46
9	25.5	medium LDL	38.95	0.14	0.37	23.28	0.23	0.97
10	23.0	small LDL	19.22	0.30	1.54	18.60	0.58	3.09
11	20.7	very small LDL	4.90	0.05	1.06	9.76	0.28	2.91
12	18.6	very small LDL	1.39	0.02	1.69	3.52	0.16	4.41
13	16.7	very small LDL	0.27	0.01	4.22	1.29	0.05	3.91
14	15.0	very large HDL	0.95	0.03	2.64	1.20	0.05	4.25
15	13.5	very large HDL	1.49	0.06	4.02	2.07	0.08	3.98
16	12.1	large HDL	20.27	0.68	3.35	11.51	0.27	2.37
17	10.9	medium HDL	24.64	0.27	1.09	14.30	0.20	1.38
18	9.8	small HDL	11.92	0.36	3.05	8.86	0.15	1.73
19	8.8	very small HDL	3.03	0.09	3.02	2.59	0.09	3.47
20	7.6	very small HDL	1.25	0.03	2.03	1.68	0.07	3.94
1–20		total	177.0	1.13	0.64	163.0	0.66	0.41
1–2	>80	CM	NA	NA	NA	5.75	0.10	1.75
3–7	30–80	VLDL	20.81	0.52	2.51	40.01	0.52	1.29
8–13	16–30	LDL	92.64	0.56	0.60	75.02	0.61	0.81
14–20	8–16	HDL	63.55	0.13	0.20	42.22	0.33	0.78

NA indicates not available; CV, coefficient of variation; CM, chylomicrons.
Pool 1, normolipidemic pooled serum (TG=56 mg/dL); Pool 2, hyperlipidemic pooled serum (TG=428mg/dL).

extraperitoneal region between skin and muscle was defined as subcutaneous fat area (SFA), with an attention range from −40 to −140 Hounsfield units. The intraperitoneal region, with the same density as SFA, was defined as the VFA. The SFA and VFA were measured at the level of the umbilicus.

Statistical Analysis

Data are expressed as mean±SD, unless stated otherwise. Correlations between various variables were presented as the Pearson correlation coefficient (r-value) with a P-value <0.05 considered to be statistically different.

Results

Clinical Characteristics and Lipid Levels of Studied Subjects

Clinical characteristics and lipid levels in 62 men in this study are shown in Table 1. A considerably wide range of anthropometric values was obtained, because they were recruited to cover a large spectrum of body fat values: body mass index (BMI) from 21 to 43 kg/cm^2, VFA from 24 to 255 cm^2, and SFA from 55 to 512 cm^2. Metabolic parameters showed a variation as compared reference values: UA from 3.8 to 12.5 mg/dL, IRI from 2 to 43 μU/mL, and PAI-1 from 5.0 to 75.7 ng/mL.

Analytical Performance of HPLC for Determination of Serum Cholesterol Levels in Major Lipoproteins and Their Subclasses

We defined 3 VLDL subclasses (large, medium, and small), 4 LDL subclasses (large, medium, small, and very small), and 5 HDL subclasses (very large, large, medium, small, and very small) on the basis of lipoprotein particle size (diameter), as shown in Table 2: chylomicrons (>80 nm, peaks 1 to 2), VLDL (30 to 80 nm, peaks 3 to 7), LDL (16 to 30 nm, peaks 8 to 13), and HDL (8 to 16 nm, peaks 14 to 20). The representative chromatograms for curve fitting analysis of normolipidemic (TC=131 mg/dL, TG=39 mg/dL) and hyperlipidemic subjects (LPL deficiency, TC=219 mg/dL, TG=1420 mg/dL) are presented in Figure 1.

Within-run reproducibility (n=5) for the cholesterol determination of 20 subclasses and major classes was determined on 2 different pooled samples (pool 1: TC=177 mg/dL, TG=56 mg/dL; pool 2: TC=163 mg/dL, TG=428 mg/dL) as shown in Table 2.

Within-run reproducibility (n=5) of LDL and HDL particle sizes was 25.20±0.07 nm (coefficient of variation [CV], 0.27%) and 11.25±0.04 nm (CV, 0.36%) for pool 1 and 25.63±0.14 nm (CV, 0.56%) and 11.03±0.05 nm (CV, 0.45%) for pool 2, respectively.

Sum area of the 20 Gaussian curves was 100.2±0.4% (99.1 to 101.7%, n=62) of the area under the original chromatogram. Sum of the peak area corresponding to HDL (peaks 14 to 20) was 99.7±1.1% (98.3 to 103.9%, n=62) of the HDL peak area under the original chromatogram.

A good correlation between HDL-C determined by the precipitation method (x) and total HDL (all HDL subclasses) by HPLC (y) was obtained: $y=0.975x+5.29$ ($r=0.973$, n=62, $P<0.0001$). Moreover, a good correlation between

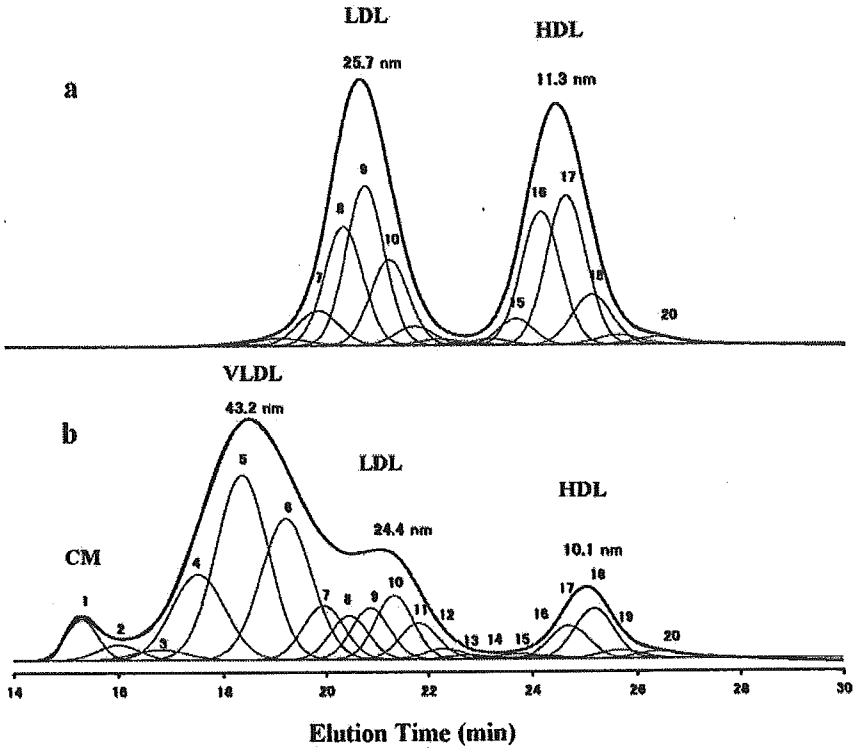

Figure 1. Representative HPLC patterns of (a) a healthy woman and (b) a patient with LPL deficiency. A 5-μL serum sample was injected onto 2 tandem gel permeation columns (TSKgel LipopropakXL) and eluted with TSKeluent LP-1 at a flow rate of 0.7 mL per min. Solid line is real HPLC pattern detected by online enzymatic reaction for TC reagent. Dashed lines are individual subclasses and their sum of Gaussian curves, which are determined curve fitting using Gaussian summation method. Serum TC and serum TG levels are 131 mg/dL and 39 mg/dL (a) and 219 mg/dL and 1420 mg/dL (b), respectively. Particle sizes (nm) determined from observed peak times are also presented.

LDL-C calculated by Friedewald equation (x) and total LDL (all LDL subclasses) by HPLC (y) was also obtained: $y=0.903x+6.28$ ($r=0.977$, n=62, $P<0.0001$).

Correlation of Cholesterol Profiles by HPLC With Clinical Parameters

Simple correlations of cholesterol levels in major lipoproteins and their subclasses with various clinical parameters (age, BMI, VFA, SFA, UA, IRI, and PAI-1) and serum TG levels are summarized in Table 3. Moreover, the correlations of LDL and HDL particle sizes are also presented in Table 3.

As for age, significant negative correlations ($P<0.01$) for medium and small HDL-C were obtained. As for BMI, significant negative correlations were observed only for HDL parameters: large HDL-C ($P<0.01$) and HDL particle size ($P<0.01$). Although no correlations were observed between SFA and all of the lipoprotein subclasses, there were significant positive correlations ($P<0.01$) of VFA with VLDL-C subclasses (large, medium, and small) and LDL-C subclasses (medium, small, and very small) and negative correlations ($P<0.01$) with large and medium HDL-C, LDL, and HDL particle sizes.

As for UA, positive correlations ($P<0.01$) for VLDL-C subclasses (medium and small) and negative correlations ($P<0.01$) for large HDL-C and HDL particle size were obtained. In the case of IRI, positive correlations ($P<0.01$) for small and very small LDL-C and negative correlations ($P<0.01$) for large HDL-C and HDL particle size were obtained. As for PAI-1, positive correlations ($P<0.01$) were observed for small HDL-C and very small HDL-C.

As for serum TG levels, there were significant positive correlations ($P<0.01$) of VFA with VLDL-C subclasses (large, medium, and small) and LDL-C subclasses (small and very small) and negative correlations ($P<0.01$) with large LDL-C, HDL-C subclasses (large and medium), LDL, and HDL particle sizes.

Influences of Traditional Lipid Parameters on the Correlation Between VFA and Lipoprotein Subclasses

Among the anthropometric values in Table 3, VFA levels showed most strong correlations with lipoprotein subclasses. Therefore, influences of traditional lipid parameters on the correlation between VFA and lipoprotein subclasses were examined by adjustment for serum TG, serum TC, HDL-C, and LDL-C levels, respectively (Table 4). Positive correlations of VFA with small LDL-C and very small LDL-C remained significant ($P<0.01$) after adjustment for TG, TC, HDL-C, and LDL-C, respectively.

As for VLDL subclasses, simple correlation analysis showed all VLDL subclasses were positively correlated with VFA, but large VLDL and small VLDL were correlated negatively and positively with VFA, respectively, after adjustment for serum TG level. In the case of LDL subclasses, adjustment for LDL-C gave a significant negative correlation ($P<0.01$) between large LDL and VFA but removed a significant positive correlation between medium LDL and VFA.

Effects of LDL-C on the Correlations Between VFA and LDL Subclasses

The studied subjects were divided into subgroups by the median value of total LDL-C levels (sum of all LDL subclasses) into the low LDL-C (n=31, LDL-C<130 mg/dL) and high LDL-C groups (n=31, LDL-C≥130 mg/dL). In the total population (n=62), a significant positive correlation